ENVIRONMENTAL RESEARCH
ECOLOGY

PURPOSE-LED PUBLISHING™

ACCEPTED MANUSCRIPT • OPEN ACCESS

Drone mapping links reindeer browsing during an herbivory pulse to divergent vegetation community responses

To cite this article before publication: Marcus P Spiegel *et al* 2025 *Environ. Res.: Ecology* in press https://doi.org/10.1088/2752-664X/adb03f

Drone mapping links reindeer browsing during an herbivory pulse to divergent vegetation community responses

Authors
Marcus P. Spiegel[1]*, Jeffrey T. Kerby[2,3,4], Dorothée Ehrich[5], Alexander Volkovitskiy[6], Alexandra Terekhina[6], Violetta Filippova[6], Kirill Shklyar[6], Natalia Sokolova[6], Aleksandr A. Sokolov[6], Marc Macias-Fauria[1,4]

Affiliations

[1]School of Geography & the Environment, University of Oxford, Oxford, OX1 3QY, United Kingdom.

[2]Aarhus Institute of Advanced Studies, Aarhus University, Aarhus 8000, Denmark

[3]Section for Ecoinformatics and Biodiversity, Department of Biology, Aarhus University, Aarhus 8000, Denmark

[4]Scott Polar Research Institute, University of Cambridge, Cambridge CB2 1ER, United Kingdom.

[5]UiT - The Arctic University of Norway, Department of Arctic and Marine Biology, 9019 Tromsø, Norway

[6]Arctic Research Station of Institute of Plant and Animal Ecology, Ural Branch, Russian Academy of Sciences, Labytnangi, Russia, 629400, Zelenaya Gorka Str., 21

*Corresponding author. Email: marcus.p.spiegel@gmail.com

Abstract

Large herbivores regulate ecosystem structure and functioning across Earth's biomes, but vegetation community responses to herbivory depend on complex interactions involving the timing and intensity of herbivory pressure and other, often abiotic, controls on vegetation. Consequently, reindeer-driven vegetation transitions in the Arctic occur heterogeneously between and even within landscapes. Here, we employed drone surveys to investigate drivers of spatial heterogeneity in vegetation responses to reindeer herbivory by mapping change comprehensively across a landscape at the fine scale inherent to plant-herbivore interactions. We conducted our surveys on the Yamal Peninsula, West Siberia in coordination with Indigenous

Nenets mobile pastoralists managing a reindeer herd of hundreds of animals, including 13 animals with GPS collars. The surveys mapped the focal landscape immediately before the herd arrived, immediately after they had left the site, and one month after the herd's activity. Using structure-from-motion (SfM) photogrammetry in a novel workflow that accounts for spatially variable uncertainty in the SfM reconstructions, we detected significant decreases in canopy height over 0.4% of the site after the herbivory event and significant increases in canopy height over 3% of the site one month later. Vegetation responses diverged depending on the amount of herbivory pressure, which was derived from the collar GPS data. In areas with higher reindeer activity, there were initial decreases in canopy height strongly suggesting trampling and defoliation, including signs of browsing around the edges of erect shrubs, and subsequent growth instead predominantly in low-lying vegetation one month later. Areas with lower herbivory pressure within the same habitat types showed strikingly little change throughout the study period. Due to our spatially comprehensive approach, we were able to pinpoint immediate and lagged effects of an herbivory pulse, ultimately demonstrating how herbivory can shape the productivity and distribution of vegetation communities within a landscape.

Introduction

Vegetation cover and biomass in the Arctic are heterogeneous across fine scales due to localised variability in abiotic determinants (Elmendorf et al., 2012; Niittynen et al., 2020; Räsänen & Virtanen, 2019; Suvanto et al., 2014) and biotic factors, including competition, mycorrhizal symbioses, and trophic dynamics (Wookey et al., 2009). Recent work has also highlighted the substantial effects of herbivores on tundra vegetation, which are mediated by abiotic conditions and vegetation type and productivity (Olofsson et al., 2013; Post et al., 2021). Within the extant

community of large herbivores in the Arctic, only reindeer and caribou (both *Rangifer tarandus*) remain widespread at high densities, although these densities (e.g., 3 kg ha^{-1} in Scandinavia) remain much lower than available estimates for large herbivores during the Late Pleistocene (e.g., 105 kg ha^{-1} in Alaska and northeastern Siberia) (Olofsson & Post, 2018). Still, their influence on vegetation has potentially broad-scale consequences for ecosystem structure and functioning throughout the tundra biome with climate feedbacks to the Earth system (Olofsson & Post, 2018; Väisänen et al., 2014). The impact of reindeer on vegetation is more complex than just their consumption of aboveground biomass, as the combination of their defoliation, trampling, and nutrient inputs from faeces/urine has been shown to promote the growth of graminoids at the expense of deciduous shrubs (Bråthen et al., 2017; Egelkraut et al., 2018; Kaarlejärvi et al., 2015; Olofsson et al., 2009). Deciduous shrubs are otherwise becoming taller and more abundant in response to climate warming, leading to greater snow trapping, ground insulation, and higher winter soil surface temperatures and, consequently, CO_2 emissions (Sturm et al., 2001). However, reindeer impacts are not spread uniformly across the Arctic or even within landscapes, and uncertainty remains regarding how vegetation responses vary over space, at different timescales following herbivory events, and as a function of the density of animals (Siewert & Olofsson, 2021).

The effects of reindeer herbivory on vegetation productivity and community composition are highly context-dependent, differing due to many factors such as the productivity of the site and the historical grazing regime (Bernes et al., 2015; Stark et al., 2023; Sundqvist et al., 2019). Remote sensing provides an opportunity to tease apart this context dependence by evaluating vegetation responses to herbivory while explicitly considering how the responses vary due to their position within the landscape and its characteristics. Most prior work using remote sensing

to study herbivory in the Arctic has focused on analysis of satellite measurements to identify the broad-scale, dominant impacts of herbivory. These analyses typically employ the normalised difference vegetation index (NDVI), a metric of vegetation greenness that is calculated using spectral reflectance data and broadly related to productivity and aboveground biomass (Raynolds et al., 2012). For example, reductions in plant biomass the year after vole and lemming peaks were visible as a decrease in NDVI over a 770 km^2 area (Olofsson et al., 2012), and similar relationships between changes in reindeer abundance and NDVI on reindeer summer pastures have also been observed (Campeau et al., 2019; Newton et al., 2014). Approaches employing remote sensing products other than NDVI have found changes in albedo and the energy balance (Cohen et al., 2013; Te Beest et al., 2016) and land cover transformation (Rees et al., 2003; Spiegel et al., 2023) as a result of reindeer herbivory. However, the coarse resolution of these analyses is not suited for explaining the observed variation and the mechanisms involved, and thus they are limited in their ability to predict how well their observations generalise to future herbivory impacts.

Drones provide the opportunity to map the impacts of herbivory at a resolution comparable to the scale at which these ecological changes occur (Senft et al., 1987). Drones can capture centimetre-resolution imagery, which has been used successfully to distinguish plant functional groups and predict plant chemistry based on spectral reflectance values in the Arctic (Thomson et al., 2021). This spatial grain is necessary to evaluate how the impact of herbivory within a landscape might vary depending on animal density, topography, habitat type, vegetation productivity, soil structure, and other ecosystem variables that are likely spatially variable within satellite pixels (Assmann et al., 2020; Siewert & Olofsson, 2020). Using an approach with repeated drone flights, one study, leveraging a strong correspondence observed between NDVI

decreases and ground truth field inventory counts of rodent impacts, found that these impacts were mediated largely by snow conditions (Siewert & Olofsson, 2021). Drone imagery has also been used to generate detailed maps of willow shrub distributions within heterogeneous plant communities on both sides of a border fence, showing the effects of different reindeer grazing regimes on shrub dynamics (Villoslada et al., 2023).

In addition to observations based on spectral reflectance measurements, remote sensing provides the capability to measure three-dimensional plant structure. Light detection and ranging (LiDAR) is an active remote sensing technology that has been widely used to quantify vegetation structure and biomass (Goetz & Dubayah, 2011; Greaves et al., 2015), but the high cost of LiDAR sensors can be a barrier and limit the temporal and spatial scales at which this technology is deployed (Cunliffe et al., 2016). Airborne LiDAR has been used to evaluate the response of forest structure to moose herbivory, but in paired exclosure-control plots rather than at the landscape scale (Petersen et al., 2023). As an alternative, structure-from-motion (SfM) can generate comparable 3D models using imagery captured with consumer-grade cameras by applying photogrammetry techniques to overlapping images capturing objects from many angles (Dandois & Ellis, 2013). Compared to the point clouds generated by LiDAR, which can include sub-canopy vegetation or terrain beneath dense canopy cover, SfM can only characterise the outer canopy surface, and the point clouds can have large uncertainties and processing artefacts depending on the survey quality (Alonzo et al., 2020; James, Robson, d'Oleire-Oltmanns, et al., 2017). Yet, with very high resolution imagery and high overlap, SfM point clouds can be 10x as dense as LiDAR point clouds, and SfM is well-suited to the open cover in most Arctic environments, where there is limited need for canopy penetration (Alonzo et al., 2020; Fraser et al., 2016). Studies in the Arctic have shown very high accuracy when comparing shrub

vegetation heights derived from SfM point clouds against ground measurements (Fraser et al., 2016), and the accuracy of SfM-modelled biomass was found to be equivalent to LiDAR models, even in the highest biomass areas (Alonzo et al., 2020), and higher than NDVI-based models (Cunliffe et al., 2020).

Conducting repeated SfM-based surveys is thus a promising approach for measuring precise changes in tundra vegetation height and biomass over time. However, simply subtracting digital surface models (DSMs) derived from the point clouds yields a noisy change product due to small differences between the DSMs caused by both physical differences, such as branch and leaf movements in the wind, and differences in the photogrammetric reconstructions, including registration errors between the point clouds and uncertainties inherent in photo-based surveys (Fraser et al., 2016; James, Robson, & Smith, 2017). Using this approach together with a shrub cutting experiment, Fraser et al. (2016) found that the change product accurately captured the extent of the cutting, but there was a nonsignificant relationship between the change in the DSMs and the amount trimmed. Furthermore, differences were detected outside the area of shrub cutting that were likely just noise.

To identify only robust change between SfM surveys, James, Robson, & Smith (2017) developed a method for topographic change detection that accounts for the spatially variable precision within SfM reconstructions and computes a variable 'level (or limit) of detection' (LoD) over space. Their LoD calculation incorporates 3D photogrammetric and georeferencing uncertainty, such that changes of a smaller magnitude than the value of the LoD at a given location are deemed not to satisfy the specified confidence level and can be discarded.

In this study, we conducted drone surveys repeated three times in summer 2021 over a 1.7 ha area on the Yamal Peninsula, West Siberia to quantify robust vegetation change in an

Arctic landscape after a reindeer herbivory event with an estimated 1,000 reindeer. Surveys were made immediately before the arrival of a reindeer herd, soon after they had left the site and migrated onwards, and again one month after the herbivory event. We coordinated the timing of our surveys and the location of the study area with the Indigenous Nenets herders managing the reindeer, 13 of which had been fitted with GPS collars. Using our SfM workflow, we quantified centimetre-resolution changes in canopy height across the landscape while assessing how this change varied with spatial differences in reindeer space use, habitat type, and initial canopy height, as well as the interactions between these variables. Our analysis examined the factors contributing to spatial heterogeneity in vegetation responses to reindeer herbivory, both in the immediate aftermath of the herbivory event and weeks later within the same growing season.

Material and Methods

Study area

We conducted our study near the Erkuta Tundra Monitoring Site in the southern part of the Yamal Peninsula, West Siberia, Russia (68.3° N, 69.0° E, Fig. 1). The vegetation cover in the area is mostly characterised as erect dwarf shrub tundra and low shrub tundra, and although the topography is generally flat, landforms such as slopes and ridges influence vegetation height and community composition (Walker et al., 2005). Within the broader area, tall thickets of willow (*Salix* spp.) and sometimes alder (*Alnus fruticosa*) reaching more than 2 m height grow in concavities and along rivers and lakes, which form a dense network subdividing the land (Ehrich et al., 2012; Hofhuis et al., 2021; V. Sokolov et al., 2012; Sokolova et al., 2014). Much of the area is underlain by ice-rich permafrost (Obu et al., 2019; Walker et al., 2009). The mean annual

precipitation is 488 mm and mean daily maximum temperature ranges from -19.7°C in January to 16.0°C in July (Karger et al., 2017, 2018).

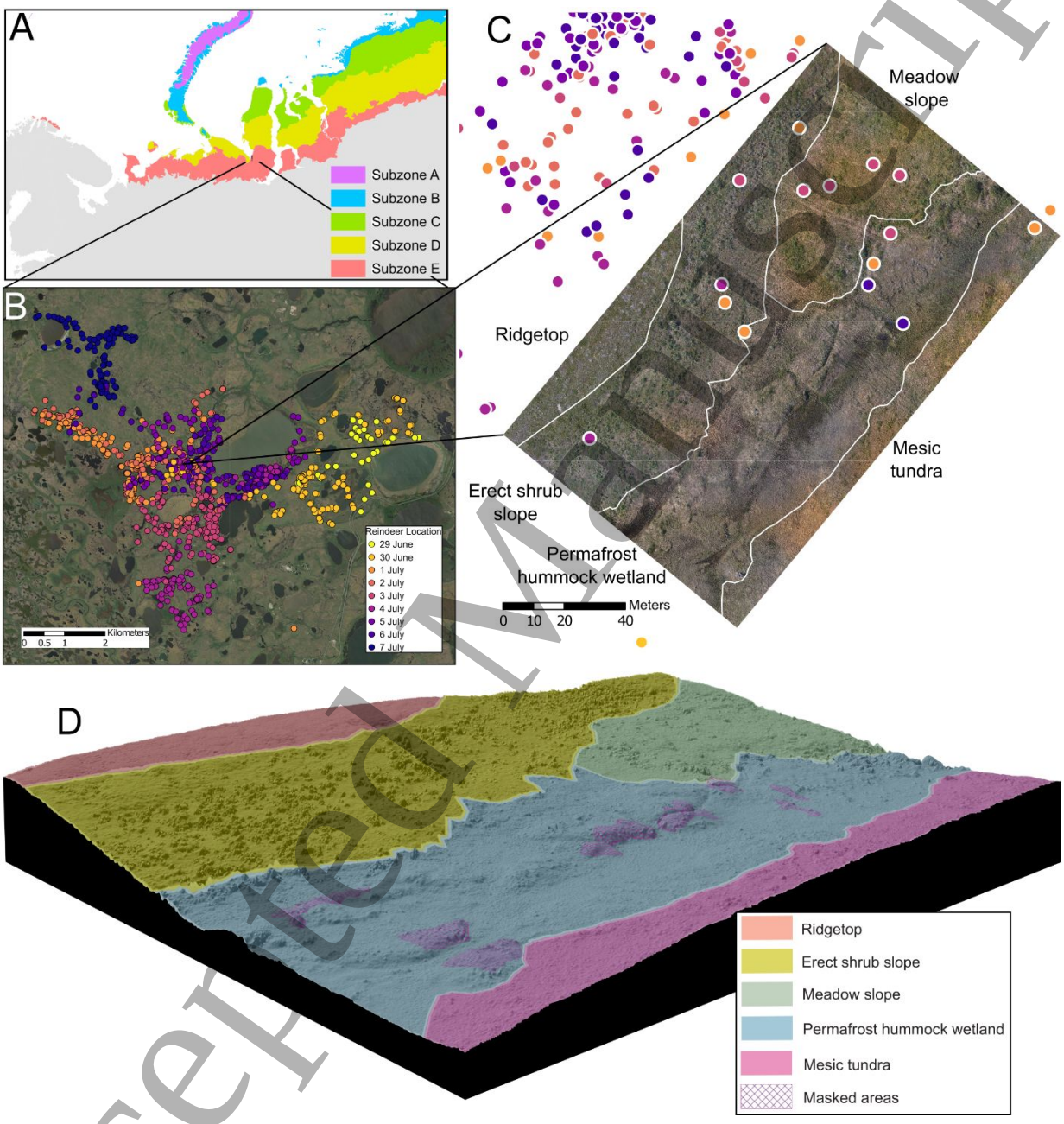

Fig. 1. The location of the study site within the Yamal Peninsula (**A-B**) and the reindeer GPS collar locations showing movements of 13 collared reindeer around the site from 29 June-7 July (**B-C**). The colour of the GPS points represents the date when the point was captured. Polygons delineate broad habitat classes (see Table S2 for descriptions) overlaid on the 30 June orthomosaic (**C**). The 3D panel (**D**) shows a representation of the land surface

based on the 30 June DSM and includes hatched polygons showing the areas within the permafrost hummock wetland that were masked from the canopy height model. The imagery base map is from ESRI and Earthstar Geographics, and the bioclimatic subzones are from the Circumpolar Arctic Vegetation map (Walker et al., 2005).

In Yamal, Indigenous Nenets herders manage the world's largest domesticated reindeer herds (~225,000 animals in total) while migrating up to 1,200 km annually (Forbes et al., 2009; Stammler, 2005; Terekhina & Volkovitskiy, 2020). The Nenets herding tradition belongs to the so-called Samoyedic type, which is common in the tundra zone of Europe and West Siberia and practised by several other ethnic groups including the Khanty and Komi-Izhma (Habeck, 2007; Istomin & Dwyer, 2021; Jernsletten & Klokov, 2002). Within the Samoyedic type, reindeer herds are large with up to several thousand animals, and herders maintain constant control over their herds. The Nenets on the southern Yamal tundra migrate every 3-5 days on average throughout the summer, which enables the rotation of seasonal pastures. While a household stays in place between movements, the herders guide the reindeer to different areas around the camp on different days (e.g., Fig. 1B), but the use of the landscape within these areas is determined by the reindeer and influenced by the forage quality and landscape structure (e.g., wind-exposed areas on ridges provide insect relief) (Skarin et al., 2020).

In the area of our study site, reindeer herds are present in all seasons (A. A. Sokolov et al., 2016). Some herds come to the area during the summer, often along long-distance migrations, whereas others are based there in the snow season. Other herbivores in the area include lemmings (*Lemmus sibiricus* and *Dicrostonyx torquatus*), voles (*Lasiopodomys gregalis, Alexandromys middendorffii, Myodes rutilus, Arvicola amphibius*), willow ptarmigan (*Lagopus lagopus*), mountain hare (*Lepus timidus*), and muskrat (*Ondatra zibethicus*) (Ehrich et al., 2012; Hofhuis et al., 2021; Sokolova et al., 2014). We chose our specific ~1.7 ha site where we

conducted our drone surveys to be adjacent to a planned campsite of a large reindeer herd passing through the area. Our team built a relationship with the herders over the past years, and we discussed their planned movements with them while designing our study. To the best of our knowledge, no other reindeer passed through the site within the period of our study, although we identified grazing marks during our initial visit indicating that some herbivory had occurred earlier in the growing season. Additionally, multiple vehicles drove through the study site after the herd had migrated onwards to collect velvet antlers from the reindeer (see Results and Discussion). The site includes a range of habitat types within a landscape that progresses from a ridgetop with bare ground and a mixture of lichens, very low stature prostrate shrubs, and graminoids, down a slope with meadow vegetation and erect dwarf birch and willow shrubs, to a sedge wetland interspersed with permafrost hummocks, and finally mesic tundra with dwarf shrubs, sedges, and a thick moss layer (Fig. 1C,D). The elevation of the study site varies from 8-17 m.a.s.l.

Drone surveys

In summer 2021, we conducted drone surveys on three dates: 30 June, before the herd migrated to the site; 7 July, just after the herd had migrated onwards; and 5 August, approximately one month after the herd had been there (Table 1). We used a DJI Phantom 4 (DJI, Shenzhen, China), a consumer-grade quadcopter with a 12.4 Megapixel RGB camera. An automated flight mission was planned using the DJI Ground Station Pro app, and the same mission was flown each time. The mission was repeated twice on each date, first to obtain nadir imagery and then with the camera angle 20° off nadir, following the protocol of (Cunliffe et al., 2020). The drone flew at a nominal 25 m.a.g.l. with 75% image overlap, such that at least 10 overlapping images captured

every part of the study site, including the edges, and the ground resolution was ~1 cm. To ensure the sharpness of the images, the "Capture Mode" was set to hover and capture at each waypoint.

We also set out 60 cm x 60 cm ground control markers, which were visible from the air and used to constrain the photogrammetric modelling. The markers were geolocated to centimetre-level precision using an RTK-GNSS survey instrument (Emlid Reach+, Emlid, Hong Kong). Five markers (one in each corner and one in the centre) were used on 30 June and four markers (one in each corner) on 7 July. Due to equipment malfunction, we were not able to geolocate ground control markers on 5 August, but instead, we found four clear features (large rocks, logs) within the photographs that had not moved over the duration of the study and used them as markers with their precise position taken from the photogrammetric models of the earlier surveys.

Table 1. Description of drone surveys and their photogrammetric models. Each survey included a flight obtaining nadir imagery and a second flight obtaining oblique (20° from nadir) imagery. All flights followed the same mission plan with prescribed waypoints, but differences in the launch point affected the true flying altitude, leading to slight variation in resolution. The automatic camera triggering during the mission skipped a waypoint or took an extra photograph in rare instances, causing small differences in the number of images captured.

Date	Local time (UTC+5)	No. of images	Ground resolution [cm/pixel]	Point density [points/cm²]	No. of dense cloud points	Reprojection error [pixels]
30 June 2021	16:49	365	0.939	1.13	350,365,588	0.278
7 July 2021	12:39	362	1.06	0.896	284,981,730	0.295
5 August 2021	14:24	363	1.09	0.849	280,955,358	0.283

Imagery processing

The drone images were initially processed in Agisoft Metashape Professional (v1.7.1) using an SfM workflow following the recommendations of (Over et al., 2021)). For each date, all images

from both the nadir and oblique flights were imported into Metashape and converted into the WGS 84 UTM zone 42N (EPSG:32642) coordinate reference system. Photos were aligned using the highest quality setting, a key point limit of 60,000, and unlimited tie points. For each survey, the alignment produced a sparse point cloud consisting of at least 1.3 million tie points representing points found in common between multiple images.

Ground control markers were added as control points to supply georeferencing information and constrain the subsequent error reduction phase of the workflow. The error reduction involves iteratively deleting low-quality tie points from the sparse point cloud and optimising the camera model, commonly known in photogrammetry as a "bundle adjustment" (Over et al., 2021). The optimisation process is sensitive to three settings used to weigh the influence of the tie points and control points: marker location accuracy, marker projection accuracy, and tie point accuracy (James, Robson, d'Oleire-Oltmanns, et al., 2017). Marker location accuracy was set to 0.02 m to account for the uncertainty in the GNSS measurements, and marker projection accuracy and tie point accuracy were initially left at the default values of 0.5 pixels and 1 pixel, respectively. Cloud points were removed based on their reconstruction uncertainty, projection accuracy, and reprojection error, and optimisation after each removal used the following lens parameters: focal length (f), principal point (cx,cy), radial distortion (k1, k2, k3), and tangential distortion (p1, p2). For each survey, after the last point removal iteration, the standard error of unit weight (SEUW) for bundle adjustment had deviated from unity, an indication of inconsistency between the error in the results and initial estimates of precision (James et al., 2020). To resolve this issue, the tie point accuracy was changed to 0.18 pixels, resulting in near-unity SEUW in each case. After completing this process, the unweighted root

mean square reprojection error, a measure of tie point quality, for all surveys was below 0.3 pixels (Table 1), which is considered ideal (Over et al., 2021).

The final optimised model contained precise estimates of the position of the camera during each image capture and the camera lens parameters. Depth maps were generated for all camera positions and a dense point cloud containing hundreds of millions of points representing all sharp features identified within each individual image was produced using the ultra high quality setting and mild depth filtering. The dense point clouds were edited by hand to remove unrealistically high and low points that are photogrammetric artefacts displaced by at least several metres from the land surface, termed "flyers" and "sinkers", and exported in the .laz format.

Robust change maps

We computed maps of robust changes comparing the first and second drone surveys from 30 June and 7 July and comparing the second survey with the third survey on 5 August. The approach used to identify significant changes in canopy height between the survey dates was based on the methodology developed by (James, Robson, & Smith, 2017) for detecting topographic change and the raster-based adaptation for detecting vegetation change created by (Graham et al., 2021) in the *sfm_gridz* package of the *SFM_Precision* repository. The procedure allows for the propagation of uncertainty in the SfM model, quantified by estimates of the precision in the tie points in the sparse point cloud, and rasterisation uncertainty, based on surface roughness.

Although the DSMs used in the change calculations (i.e., the subtraction of DSMs produced after and before a given event) are based on the dense point clouds, the dense matching

process does not alter the optimised image network, so the precision of the surface model is mainly derived from the tie point precision (James, Robson, & Smith, 2017). Both James, Robson, & Smith (2017) and Graham et al. (2021) used a Monte Carlo procedure to obtain the precision estimates, but more recent versions of Metashape enable precision estimates to be calculated directly from the bundle adjustment within the software (James et al., 2020). When rasterising the dense point clouds into DSMs and the sparse point cloud precision estimates into precision rasters, pixel resolution was chosen to be fine enough to retain the detailed spatial variation captured by the points, but not so fine that the rasters would be noisy and require extensive gap filling. This resulted in the rasterisation of the DSMs from the dense point cloud at 5 cm pixel resolution, compared to the ~1 cm ground resolution of the surveys, using the mean point height within each pixel. The standard deviation of point heights within each pixel was taken as the DSM roughness. The precision rasters were calculated at a coarser 10 cm resolution, given that they were derived from the sparse point cloud, and gaps were filled by the maximum (worst) precision estimate within each point cloud, providing a conservative estimate of the uncertainty in the photogrammetric reconstruction in these areas (Fig. S1). Although the difference in resolution between the precision rasters and DSMs implies that the reconstruction uncertainty was not uniquely quantified at every pixel in the DSMs (i.e., each block of four 5 cm DSM pixels was associated with just one 10 cm precision raster pixel), this spatially variable uncertainty is a substantial improvement over approaches that rely on a single value to characterise the overall reconstruction uncertainty for a DSM.

The spatially variable limit of detection (LoD) for significant changes between two repeated surveys was calculated at 5 cm resolution as:

$$LoD = t\sqrt{(R_1 + P_1)^2 + (R_2 + P_2)^2 + reg^2} \quad (1)$$

where t is an appropriate scalar value for the required confidence level, R_1 and R_2 are the DSM roughness rasters, P_1 and P_2 are the precision rasters, and reg is the overall registration error between surveys (Fig. S2). Based on the t distribution, we chose t=1.96 to represent a 95% confidence level, and *reg* was taken as 0, as all surveys were defined from the same datum and georeferencing uncertainty is included within P_1 and P_2 (James, Robson, & Smith, 2017). Finally, robust canopy height change maps were produced by subtracting the DSMs but retaining only differences exceeding the LoD at the location of the change.

Habitat delineation

We manually divided the study site into broad habitat classifications based on habitat descriptions while in the field and visual inspection of the orthomosaics and DSMs (Fig. 1C,D). The ~1 cm resolution orthomosaics have sufficient detail to distinguish plant functional types (i.e., differentiating between erect shrubs, dense graminoids, and sparser low-lying vegetation). At 10 locations chosen across the study site to cover a variety of vegetation communities, we described the habitat type and noted the dominant species or plant groups using groups similar to the plant functional types defined by (Bråthen et al., 2007) (Fig. S3, Table S1). Six of the locations were described on 30 June and four on 7 July, and each was geolocated precisely using the GNSS. We compared our field observations with the drone-derived products and delineated five broad habitats characterised by their landscape position and vegetation: ridgetop, erect shrub slope, meadow slope, permafrost hummock wetland, and mesic tundra (see Table S2 for descriptions). These habitat classifications were used to identify where canopy change was occurring in the landscape and to evaluate the spatial heterogeneity in plant responses within similar vegetation communities.

Canopy height modelling

To compute canopy height, we took the difference between the elevation values within the DSM from each survey date and a digital terrain model (DTM) that we generated from the dense point cloud from the 7 July survey. This survey was chosen as the basis for the DTM because on this date we also walked transects across the study site with the GNSS, recording terrain points approximately every 10 m to give a total of 162 points for validation of the DTM (Fig. S4). We derived the DTM using the cloth simulation filtering (CSF) algorithm implemented in the LidR package in R (Roussel et al., 2020; Roussel & Auty, 2021), which turns the original point cloud upside down and then drapes a cloth over the inverted surface from above to distinguish which points belong to the terrain (Zhang et al., 2016). The algorithm relies on the choice of three parameters that govern how the cloth interacts with the point cloud: "class_threshold," "cloth_resolution," and "rigidness." To choose these parameters, we first coarsely tuned the values while visually assessing the resulting DTM, and then fine-tuned the values while calculating the root-mean-square error (RMSE) and mean error using the GNSS points for validation. We found a tradeoff between minimising these two errors, indicating that a model that fit the points better (lower RMSE) would have higher bias (i.e., mean error was always positive, so higher values implied that the DTM tended to be further above the true terrain). We selected a Pareto-optimal combination of parameters (class_threshold=0.01 [m], cloth_resolution=0.45 [m], rigidness=3) that produced a reasonable DTM upon visual inspection with an RMSE of 11 cm and mean error of 2.5 cm (Fig. S4). The canopy height models (CHM) were computed as the difference between the DSM for each survey and this DTM, but we found that some permafrost hummocks, rather than the vegetation growing on them, were characterised as part of the canopy due to their particular geomorphology within the landscape. For analyses incorporating the CHMs, we masked out these areas to avoid introducing further error (Figs. 1,

S4); in any case, they include very little area with robust change (0.15 m^2 after herbivory, 2.8 m^2 one month later).

Reindeer space use intensity

We estimate that there were roughly 1,000 reindeer in the herd passing through our study site over the course of six days. Thirteen of these animals had been fitted with Lotek Litetrack Iridium 420 GPS collars (Lotek Wireless Inc., Newmarket, ON, Canada), which recorded their positions every 1.5 hours from 30 June to 7 July 2021 (Terekhina et al., 2022). The collar weighs 400-450 g depending on the length of the strap, making up less than 1% of animal body weight. The accuracy of each fix was assessed using the dilution of precision (DOP). DOP is an indicator of the quality of a GPS position and is based on the number of satellites used, each satellite's location relative to the other satellites in the constellation, and their geometry in relation to the GPS receiver. All GPS fixes we received had DOP values lower than 7, implying an accuracy of 4-14 m (Jung et al., 2018). The GPS data show that the herd moved to their campsite adjacent to our study site on 30 June in the late evening after we had visited the site, remained there until 6 July, and by 7 July, had moved onto their next campsite (Fig. 1B).

To quantify the spatial variation in the reindeer activity across the study site, we calculated the integrated proximity of each pixel *i* showing significant canopy height change to the *n*=212 reindeer collar points within 100 m of the study site as:

$$Integrated\ proximity_i = \sum_{j=1}^{n} \frac{1}{(Euclidean\ distance)_{ij}} \quad (2)$$

We also computed how the integrated proximity to reindeer varies over the whole study site (Fig. S5) to enable comparison between the distribution in this metric within the change pixels and the wider distribution within all pixels in the study site.

Statistical analyses

We analysed the factors influencing where significant changes in canopy height were occurring within the landscape by comparing the distributions of variables for just the change pixels against all pixels while controlling for habitat type. To assess whether change was occurring primarily in certain vegetation types (e.g., tall or low-lying vegetation), we tested whether the distributions of canopy heights diverged in pixels with significant change, and to assess the influence of reindeer, we tested whether significant changes occurred in higher proximity to reindeer. We conducted these tests using the Kolmogorov-Smirnov goodness-of-fit test using the ks.test function from the dgof package (Arnold & Emerson, 2011) in R.

Results

Maps of significant canopy height change

Significant canopy height changes (i.e., differences exceeding the LoD) occurred only within specific areas of the site, while large swathes showed no significant change (Fig. 2). Comparing the observations immediately before and after the herd was present on the site, the total area of significant change was 66.6 m^2 (0.403% of the study site), of which 60.8 m^2 (91.3% of the changed area) showed height decreases. One month later, canopy height had changed significantly across 489 m^2 (2.96% of the study site), of which 462 m^2 (94.5% of the changed area) increased in height since immediately after the herd had left. Assessed visually, the most concentrated changes observed immediately after the reindeer herbivory event were significant

decreases in the height of both erect shrubs and low-lying graminoids and forbs in the habitats on the sloped area, primarily towards the northeast and closer to the campsite. The height decreases detected on the erect shrubs were often only around their lateral extents, appearing doughnut-shaped in the change map (Fig. 2). Large stretches of vegetation, mostly sedges, within the wet topographic lows showed significant increases in height one month later, but there was also significant growth in the same sloped area where decreases were observed immediately after the herd had left, primarily where there was low-lying vegetation around the erect shrubs (i.e., not in the same pixels where a height loss was detected immediately after the herbivory event). Pixels where vegetation both significantly decreased in height after the herbivory event and significantly increased one month later comprised 15.1 m^2 of the site, or 22.6% of the initial decreases and 3.26% of the subsequent growth.

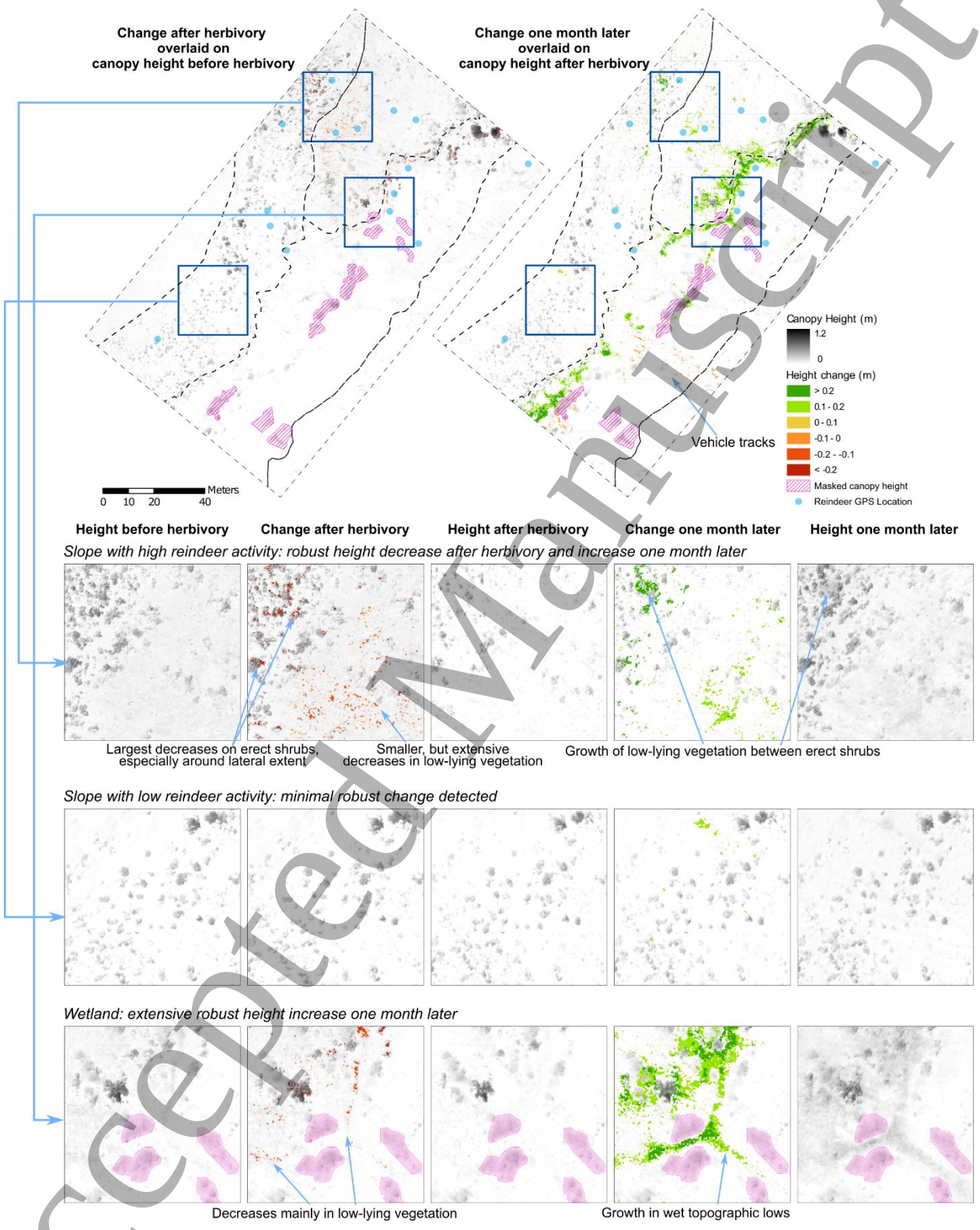

Fig. 2. Maps showing the significant changes in canopy height detected immediately after the herd had left the site and one month later. The changes are overlaid on the canopy height model from the drone survey preceding the

change. Reindeer collar GPS points within the study site are displayed. Hatched polygons show areas that were masked out in analyses involving canopy height due to mischaracterisation of permafrost hummocks as part of the vegetation canopy (see Methods). Vehicle tracks that were identified as significant decreases in canopy height one month later are indicated in the full map of change one month later. Three areas within the site are enlarged and annotated for more detailed comparison of the products from the drone surveys at these locations.

Comparison between habitat types

The significant canopy change was distributed unevenly between habitat types. The ridgetop and mesic tundra had minimal change area, so the analysis focused on the remaining habitat types. Immediately after the herbivory event, the meadow slope had the most area (29.3 m^2, 1.1% of habitat area) where canopy height decreased, but the average magnitude of that change was only 14.0 ± 9.1 cm (± SD) (Fig. 3A,C). Significant decreases also occurred over a substantial area on the erect shrub slope and permafrost hummock wetland, 15.5 m^2 (0.34% of habitat) and 15.7 m^2 (0.25% of habitat), respectively, with the largest average decrease of 32.7 ± 10.7 cm on the erect shrub slope. Of the habitat types, only the permafrost hummock wetland had more than 1 m^2 significantly increase in height, showing an average increase of 8.19 ± 2.4 cm over 5.57 m^2 (0.089% of habitat).

One month later, the majority of significant increase, 296 m^2 (4.8% of habitat), was on the permafrost wetland, followed by 128 m^2 (4.7% of habitat) on the meadow slope and 36.6 m^2 (0.80% of habitat) on the erect shrub slope (Fig. 3B). The average magnitude of the growth was similar in each of these three habitat types, 23.1 ± 14.9 cm, 16.7 ± 6.7 cm, and 19.6 ± 6.1 cm on the erect shrub slope, meadow slope, and permafrost hummock wetland, respectively (Fig. 3D). Significant decreases were primarily detected on the permafrost hummock wetland and mesic tundra, both with an average magnitude less than 10 cm. These decreases were concentrated

mostly in the tracks of the vehicles that drove through the study site to collect reindeer antlers (Fig. 2).

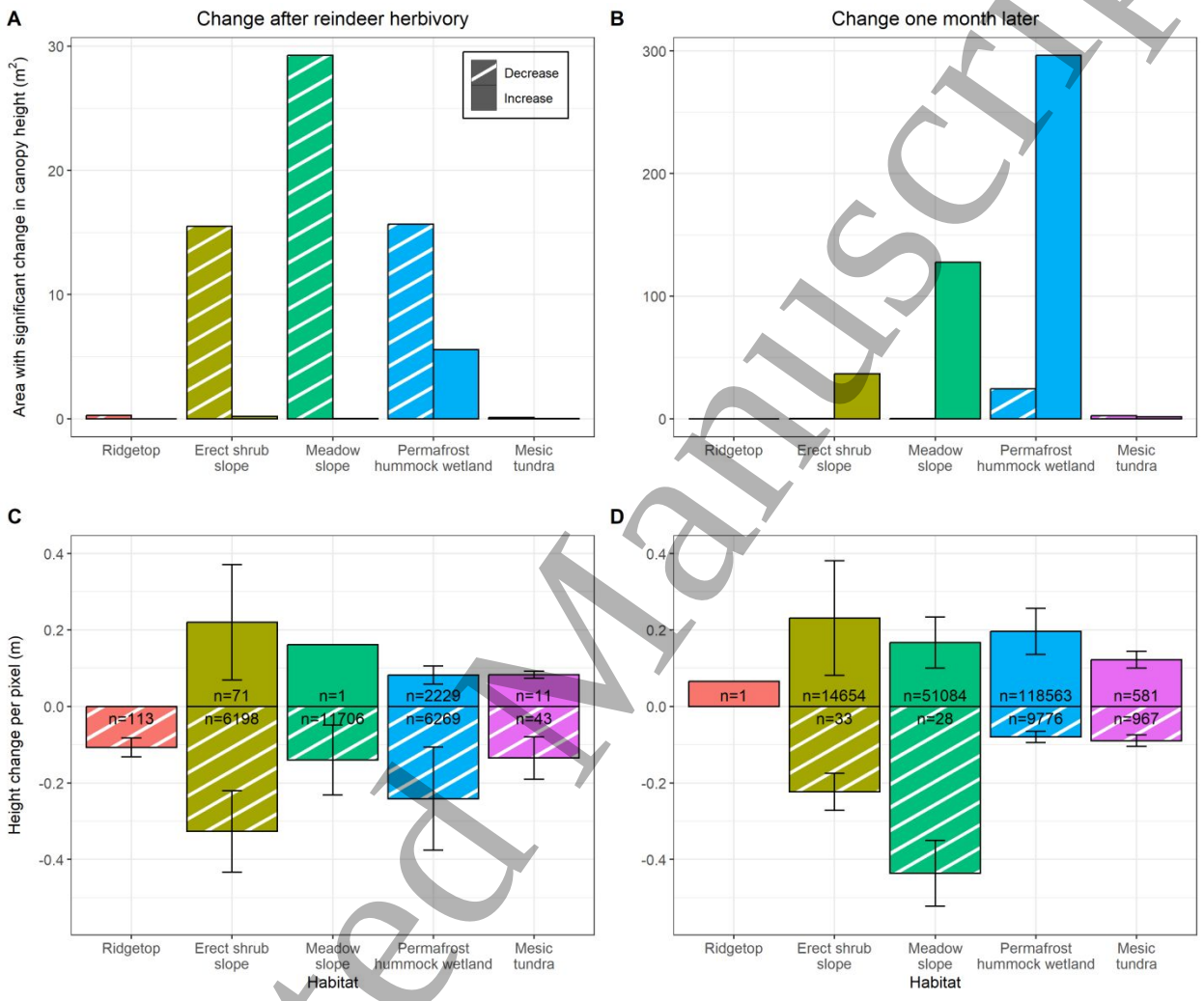

Fig. 3. Immediate and delayed areas of significant change (**A,B**) and mean height of this significant change per pixel (**C,D**) within different habitat types. The bars are coloured to correspond to the colouring of habitat types in Fig. 1. Change is separated into height increases (solid) and decreases (white stripes). Error bars represent ± standard deviation, and the number of change pixels is given within the bars. Note the difference in the scales for the change area in the different time periods (**A**,**B**).

Distribution of canopy heights where significant change occurred

The different habitat types varied in their distributions of canopy heights, reflecting differences in the abundances of tall (i.e., erect shrubs) and low-lying (i.e., lichens, prostrate shrubs, graminoids) vegetation. Evaluating the distributions of canopy heights specifically for the pixels where significant changes occurred and comparing these distributions to the initial heights of all pixels within each habitat type suggested whether changes were concentrated within particular vegetation types (Fig. 4). Before the herd arrived, the median canopy height was 1.33 (25^{th}-75^{th} percentile: 0-5.56) cm in the erect shrub slope, 5.15 (3.14-7.70) cm in the meadow slope, and 0.00 (0-1.12) cm in the permafrost hummock wetland (Fig. 4A). For all three habitat types, the pixels showing significant height decreases after the herbivory event were concentrated within initially taller vegetation, but to varying degrees. The significant decreases in the erect shrub slope had the tallest median initial canopy height at 33.2 (25.7-42.0) cm, consistent with decreases primarily in erect shrubs (Fig. 4C). The pixels with significant decreases in the permafrost hummock wetland had a median height of 24.4 (12.9-43.9) cm, and the meadow slope had a median height of 10.2 (8.68-13.6) cm in these pixels. Kolmogorov-Smirnov goodness-of-fit tests indicated that the distribution of canopy heights of change pixels diverged significantly from the distribution of all pixels for all habitat types (Table 2).

Immediately after the herd had left, the distribution of canopy heights had shifted toward lower heights (Fig. 4B). Across all habitat types, the pixels showing a significant increase one month later were predominantly in low-lying vegetation (Table 2). Over 52% of these pixels had an initial canopy height of 0, indicating that their elevation was taken as the level of the terrain in the generation of the DTM used for computing canopy height for all three surveys. A canopy height of 0 does not necessarily indicate no vegetation, but rather reflects that some of the 7 July DSM was interpreted as terrain even if it was low-lying vegetation, due to the limited penetration

of the canopy with SfM. The median height in pixels showing a significant increase was barely greater than 0 in the erect shrub slope (0.11 (0-1.47) cm), meadow slope (0.07 (0-1.11) cm), and permafrost hummock wetland (0.00 (0-0.55) cm) (Fig. 4D). However, examining the right tail of the distributions informed to what extent increases occurred in initially taller vegetation in addition to low-lying vegetation. The erect shrub slope had the highest percentage of its total area, 7.26%, covered by vegetation with a canopy height greater than 10 cm, but only 2.39% of the area that showed significant increases in height one month later had vegetation taller than 10 cm. In the meadow slope, 5.08% of the canopy in the full habitat was above 10 cm compared to 3.90% of the pixels with significant increases, and in the permafrost hummock wetland, 3.44% of the canopy was above 10 cm compared to 1.06% of the pixels with significant increases. Thus, the concentration of significant increases predominantly in low-lying vegetation was less pronounced in the meadow slope than in the permafrost hummock wetland and, especially, the erect shrub slope. Whereas significant decreases in the erect shrub slope immediately after the herbivory event tended to be detected in the taller vegetation, one month later, significant height increases were concentrated where the vegetation had been shorter initially within this habitat type. This pattern was true, but to a lesser extent, in the permafrost hummock wetland, and was much less pronounced in the meadow slope.

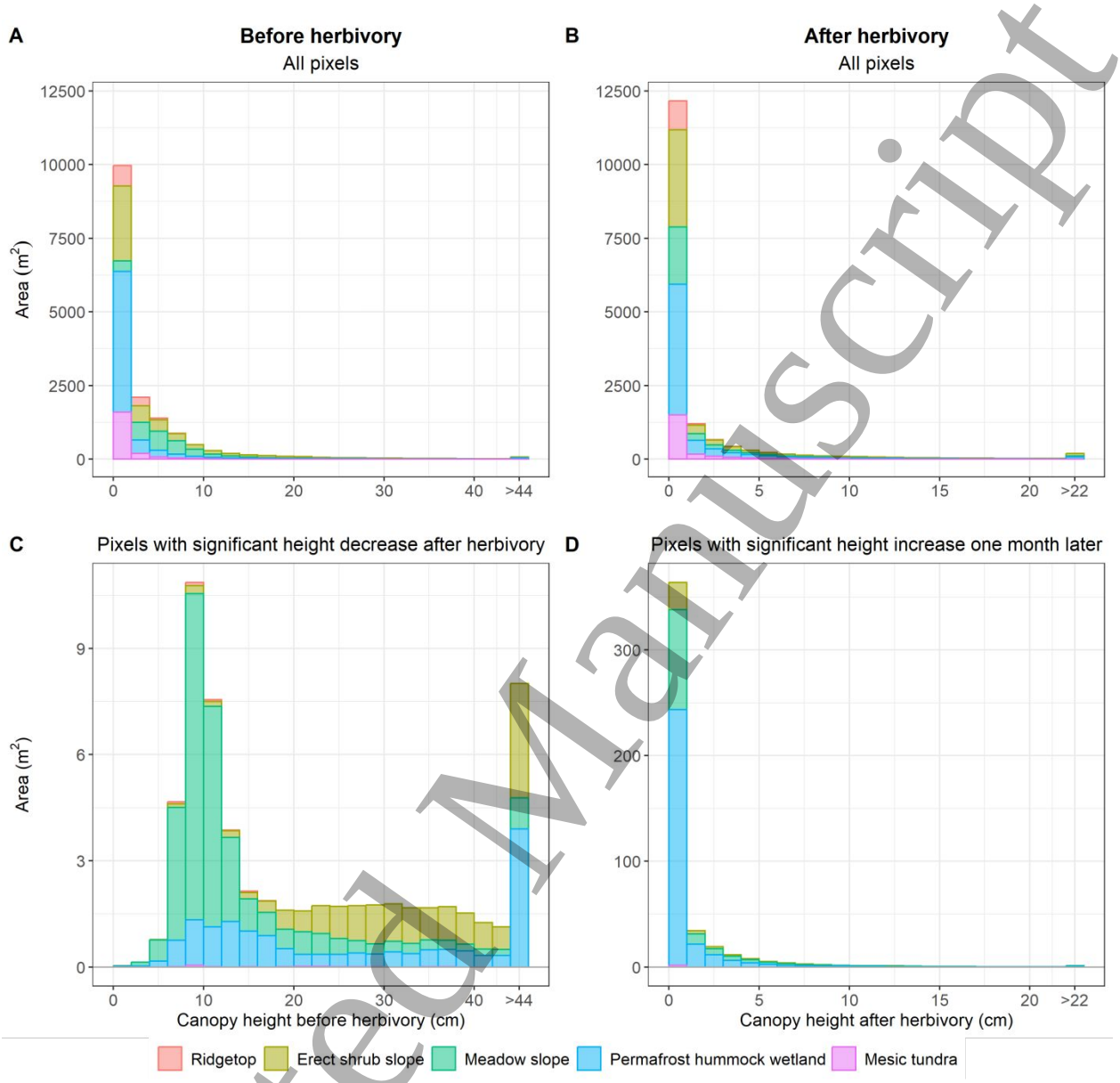

Fig. 4. Comparison between the distribution of initial canopy height in pixels with significant canopy height change and the full distribution of canopy height within each habitat type. All pixels in the study site are categorised by habitat type and binned by canopy height before the herbivory event in **A** and after the herd had left in **B**. The subset of pixels in **A** with significant canopy height decrease detected after herbivory are shown in **C**, and the subset of pixels in **B** with significant increase one month later are shown in **D**.

Table 2. Results of Kolmogorov-Smirnov tests evaluating divergence in the canopy height of the significant change pixels compared to all pixels across each habitat type. The comparisons were performed separately for decreases in height during the herbivory event and increases in height occurring in the following one month. Due to the fine pixel

resolution (400 pixels/m^2), sample sizes of the change pixels were large, increasing the likelihood that small differences in the distributions were significant according to the p-values. Higher values of the test statistic *D* indicate greater divergence from the null distribution, although the magnitude of the divergence should be interpreted while considering the area of significant change.

	Canopy height before herbivory					Canopy height after herbivory				
	All pixels	Pixels with significant decrease in height after herbivory				All pixels	Pixels with significant increase in height one month later			
Habitat	Median canopy height (cm)	Median canopy height (cm)	Height decrease area (m^2)	Test statistic *D*	*p*	Median canopy height (cm)	Median canopy height (cm)	Height increase area (m^2)	Test statistic *D*	*p*
Ridgetop	1.41	9.60	0.28	0.97	<0.01	0.03	0.00	0.00	-	-
Erect shrub slope	1.33	33.20	15.50	0.86	<0.01	0.12	0.11	36.64	0.05	<0.01
Meadow slope	5.15	10.22	29.27	0.64	<0.01	0.15	0.07	127.71	0.05	<0.01
Permafrost hummock wetland	0.00	24.44	15.64	0.91	<0.01	0.12	0.00	295.62	0.14	<0.01
Mesic tundra	0.00	14.44	0.11	0.93	<0.01	0.11	0.00	1.45	0.22	<0.01

Influence of reindeer space use intensity within habitat types

The significant height changes varied in the strength of their association with the space use intensity of the reindeer herd. After the herbivory event, the height decreases that were detected in the erect shrub slope were especially concentrated where the integrated proximity to reindeer was higher, typically above 3 m^{-1} (Fig. 5B), even though much of the erect shrub slope had lower reindeer activity (Fig. 5A, integrated proximity around 2 m^{-1}). This divergence is evident in the Kolmogorov-Smirnov tests, in which the erect shrub slope had the highest *D* value (0.55) among habitat types with more than 1 m^2 of significant change during the herbivory event, implying that change in the erect shrub slope was most biased towards higher reindeer pressure (Table 3). Significant decreases also tended to occur where there was higher reindeer activity within the meadow slope and, to some extent, within the permafrost hummock wetland.

The influence of the reindeer herd was less clear in the significant growth observed one month later. Here, the changes in the permafrost hummock wetland and the meadow slope did not seem to be predominantly in the areas with higher reindeer activity, as the distributions of integrated proximity for the change pixels (Fig. 5C) resembled the full distributions over the habitat types (Fig. 5A). Although there were fewer pixels showing significant increases in the erect shrub slope, these were concentrated again in areas with higher integrated proximity, and this habitat type similarly had the highest *D* value (0.42) in the Kolmogorov-Smirnov tests (Table 3). Where reindeer activity was higher with integrated proximity above 3 m^{-1} in the erect shrub slope, the median height increase was 23.4 cm, but a substantial proportion of the detected growth, 35.3%, was less than 10 cm. These smaller height increases occurred where there was low-lying vegetation.

Table 3. Results of Kolmogorov-Smirnov tests evaluating divergence in the integrated proximity to reindeer of the significant change pixels compared to all pixels across each habitat type. Pixels with significant change during the herbivory event and one month later were separately compared to the same null distribution of integrated proximity values. Due to the fine pixel resolution (400 pixels/m^2), sample sizes of the change pixels were large, increasing the likelihood that small differences in the distributions were significant according to the p-values. Higher values of the test statistic *D* indicate greater divergence from the null distribution, although the magnitude of the divergence should be interpreted while considering the area of significant change.

	All pixels	Change after reindeer herbivory				Change one month later			
Habitat	Median integrated proximity (m^{-1})	Median integrated proximity (m^{-1})	Change area (m^2)	Test statistic *D*	*p*	Median integrated proximity (m^{-1})	Change area (m^2)	Test statistic *D*	*p*
Ridgetop	2.66	2.24	0.28	0.82	<0.01	3.76	0.00	-	-
Erect shrub slope	2.70	3.79	15.67	0.55	<0.01	3.63	36.72	0.42	<0.01
Meadow slope	2.75	3.08	29.27	0.32	<0.01	2.63	127.78	0.29	<0.01
Permafrost hummock wetland	1.92	2.11	21.25	0.27	<0.01	2.04	320.85	0.25	<0.01

Mesic tundra	1.70	1.73	0.14	0.36	<0.01	1.60	3.87	0.32	<0.01

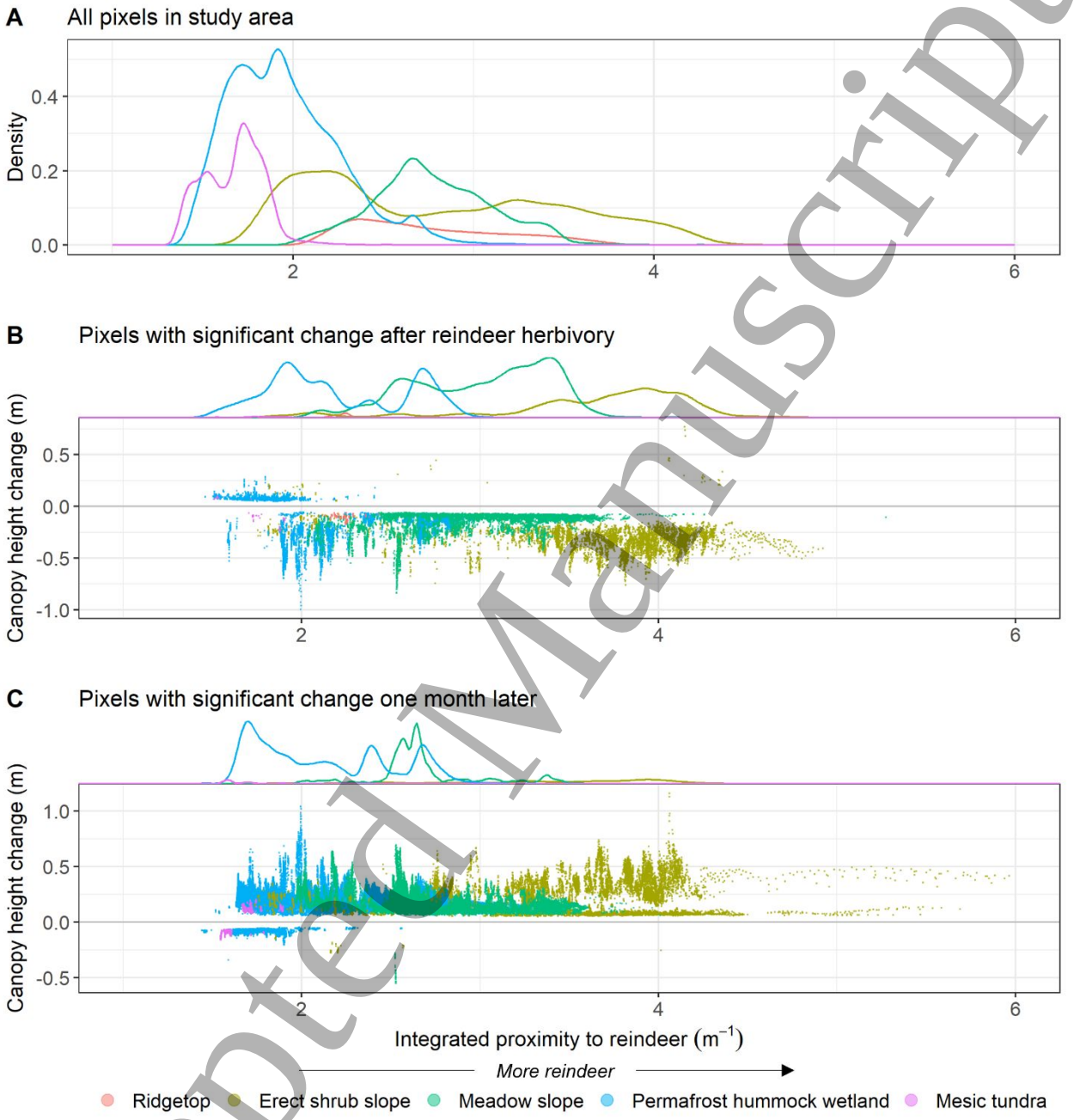

Fig. 5. Relationship between the level of reindeer herbivory pressure and the presence and magnitude of significant canopy height changes within each habitat type. For comparison, the density plot in **A** depicts how all pixels in each habitat type are distributed along the integrated proximity to reindeer metric. Higher x-axis values indicate areas with higher reindeer space use intensity. The canopy height change for each pixel showing significant change after the herbivory event (**B**) and one month later (**C**) is plotted against integrated proximity to reindeer, and density plots

above the scatterplots show how the significant change pixels are distributed within this metric. The comparison of the overall distributions in (**A**) against the distributions where significant changes were detected in (**B**) and (**C**) enables analysis of the tendency for detected changes in vegetation height to occur in association with higher reindeer pressure.

Discussion

We examined spatial heterogeneity in vegetation change after a pulse of herbivory from a herd of reindeer in a tundra environment using a novel photogrammetric approach. Although this methodology for robust change detection has been used successfully in geomorphological applications (James et al., 2020; James, Robson, & Smith, 2017), its adaptation for detecting vegetation change is new (Graham et al., 2021). In this study, we were able to identify significant, centimetre-precision changes in canopy height and pinpoint where they occurred within the landscape using a consumer-grade quadcopter. This methodology allowed us to not only create new landscape maps, but also address ecological questions by analysing vegetation change with both fine detail and systematic landscape coverage. Our analysis showed significant changes over a small fraction of the study site, less than 1% immediately after the reindeer herbivory pulse and less than 3% one month later. Yet, as expected, nearly all the changes in the week between the arrival of the herd and its departure were significant height decreases that we have linked to reindeer activity. In contrast, vegetation growth was the predominant detectable change one month after the reindeer herbivory pulse, which coincided with the peak of the growing season. This result provides confidence that the canopy height differences we mapped were robust signal rather than noise resulting from the intricate nature of the vegetation or photogrammetric error (Fraser et al., 2016).

The area and magnitude of detected change varied substantially across the study site. Even within the same habitat type, some areas exhibited extensive change whereas others showed almost no change and were nearly indistinguishable in the DSMs of the three surveys (Fig. 2). We assessed how the habitat type interacted with reindeer herbivory pressure and the initial canopy height of the vegetation in driving this spatial heterogeneity in responses. The collar GPS points falling within the study site were mostly towards the north of the site and within areas of the erect shrub slope, meadow slope, and permafrost hummock wetland (Figs. 1C, 2). The variation in reindeer space use intensity within the habitat types facilitated disentangling the role of habitat type and herbivory in driving canopy height changes (Fig. S5). Although only 13 of the roughly 1,000 reindeer in the herd were collared, reindeer are a very gregarious species, especially when domesticated, and animals within a group typically show highly synchronous behaviour (Colman et al., 2004). Therefore, the 15 collar GPS points falling within our study site (Fig. 1C) likely each represent considerably more herbivory pressure than just a single reindeer. These points were recorded from seven different reindeer on four different dates from 1 July to 6 July, indicating that there was substantial pressure from the herd throughout the period between our first two surveys. In addition, our site was located just next to the campsite, where reindeer tend to spend much of their time in search of relief from insect harassment, especially in July (Terekhina et al., 2022). Accordingly, on our second visit we saw clear signs of recent presence of a considerable number of reindeer in the form of fresh faeces, hoofprints in humid places, trampled vegetation, shed hair, and browsing marks on shrubs (Fig. S8).

The significant decreases in canopy height after the herbivory event were found in the erect shrub slope, meadow slope, and permafrost hummock wetland. Within each of these habitat

types, the change predominantly occurred in areas with higher herbivory pressure based on our measure of reindeer space use (Fig. 5, Table 3). The greatest area of change was in the meadow slope, where the decreases in canopy height were typically of small magnitude and affecting vegetation that was already low-lying (Figs. 3, 4). This low-lying vegetation was likely not only grazed, but also trampled by reindeer. While trampling causes a reduction in canopy height, it does not necessarily indicate a loss of biomass, as the vegetation, and potentially the active layer, may just be compressed down. However, beyond this physical impact, trampling by large herbivores can cause shifts in vegetation community composition by damaging plants, creating gaps for seedling establishment, and altering soil properties (Egelkraut et al., 2020; Olofsson et al., 2001; Tuomi et al., 2020; van der Wal, 2006). Moreover, Nenets herders typically direct their reindeer so that grazing and browsing primarily take place not in the immediate vicinity of the campsite. Where our site was located adjacent to the campsite, trampling is expected to be a key physical impact from the reindeer's activities, such as the daily corrals (round-ups) of all reindeer to rotate draught animals.

In contrast, the significant decreases in canopy height in the erect shrub slope covered a smaller area and were, on average, larger changes in initially taller vegetation (Figs. 3, 4, Table 2). These changes likely represent reindeer browsing around the edges of erect shrubs, illustrating how reindeer herbivory can prevent shrub infilling via lateral growth, one of the ways in which shrub expansion is occurring across the Arctic (Myers-Smith et al., 2011). While these shrubs are small enough, reindeer can keep them in a browse trap and limit their growth, maintaining the open state of the vegetation (Bråthen et al., 2017). This reindeer effect works towards counteracting the likely tendency for shrub expansion at our study site, as predicted especially in the low Arctic and observed elsewhere in the region (Epstein et al., 2004; Macias-

Fauria et al., 2012; Myers-Smith et al., 2015), although our study cannot quantify this effect. In the permafrost hummock wetland, the significant decreases were a combination of the impacts on low-lying vegetation and erect shrubs detected in the meadow slope and erect shrub slope, resulting in an average height decrease that was intermediate in comparison (Figs. 2, 3).One limitation of our raster-based approach is that it does not indicate whether the decreases in canopy height represent the vegetation initially present becoming shorter or a reduction in the lateral extent of the crowns of taller vegetation revealing the terrain or understory below. We believe that the significant height decreases we detected include both types of changes, primarily contraction of the crown in erect shrubs and height reduction of the low-lying vegetation. Classifying vegetation into functional types based on point clouds and/or by incorporating additional spectral information has been achieved with high accuracy in the Arctic (Orndahl et al., 2022; Thomson et al., 2021; Yang et al., 2021) and could be incorporated into the workflow to differentiate between these changes. Without this differentiation, and due to the potential physical impacts of trampling already mentioned, conversions of canopy height change into biomass loss would need to account for this uncertainty.

In the month between the herbivory event and our final survey, the growing season reached its peak, causing increases in canopy height across the site. The progression of vegetation growth through the peak growing season complicates our interpretation of whether detected changes were linked to herbivory, and in many areas the spatial distribution of changes was linked to other landscape features. In particular, substantial growth occurred in wet topographic lows across the permafrost hummock wetland in areas with and without reindeer activity (Fig. 2). However, in certain habitat types, changes were skewed towards areas with higher reindeer space use intensity. In the erect shrub slope, in areas in closer proximity to

reindeer activity, there were significant height increases, but in contrast with the significant decreases after herbivory, these increases were concentrated on places initially covered by low-lying vegetation. Some growth in taller vegetation likely was not detected due to the higher roughness, and consequently LoD, limiting the changes that qualified as significant in these areas. Where larger magnitude growth was detected, some likely represented the lateral expansion of the crowns of erect shrubs, some of which may have recovered from browsing and continued to grow, as has been observed previously in deciduous shrubs following defoliation (Chapin III, 1980; Chapin III et al., 1980). We observed this lateral expansion in cases where the same pixel had a significant decrease around the edge of a tall shrub after the herbivory event and then a significant increase one month later. Yet, a more substantial portion of the growth in the month after the herbivory pulse occurred directly in the low-lying vegetation (Fig. 2).

One potential caveat is that some component of these detected height increases may not have been entirely due to vegetation growth but may instead represent physical vegetation rebound after trampling. However, even when directly comparing the first drone survey before the herbivory event to the final survey one month later, we found significant changes showing an increase in canopy height between the erect shrubs (Fig. S6). Additionally, our observations in the field and of the RGB imagery showed only sparse vegetation between the erect shrubs before the reindeer arrival in June and abundant graminoids during our final visit in August. Although we do not rule out that some rebound may have occurred, these findings indicate that substantial vegetation growth did occur where our height modelling detected significant change and suggest that this is the likely process driving the detected change in canopy height. Notably, this growth occurred only where there was higher reindeer activity, whereas no significant change was detected in other areas of the erect shrub slope (Fig. 2, 5), potentially demonstrating that reindeer

activity can not only prevent the infilling of shrubs as seen above, but promote grassland vegetation growth, even within a single growing season after an intense pulse event lasting a few days.

Although our study covers just one site where reindeer impact was concentrated directly adjacent to a campsite, it provides an evidence point at a heretofore unreported scale supporting that reindeer are ecosystem engineers in the region, as similar densities of reindeer are present within comparable landscapes across Yamal during the growing season. Our findings also empirically highlight that the impact of reindeer is not confined to their consumption, but that their trampling and potentially also nutrient inputs via faeces and urine can have significant effects on plant growth and community composition across levels of landscape heterogeneity (Forbes et al., 2009; Olofsson et al., 2004). An important consideration is whether the changes we detected are temporary or long-lasting. Without data collection over multiple years, we cannot definitively evaluate this question, and there are examples in the literature where the effects of herbivory pulses are found to be short term (Jefferies et al., 1994) and more persistent (e.g. Forbes et al., 2009). In our robust comparison of the initial drone survey with the final survey (Fig. S6), most of the significant changes linked to reindeer were not present, suggesting a potential offsetting of the significant decreases during herbivory and the significant increases in the month after. However, considering the full extent of the differences in the DSMs rather than just the significant differences over this time period (Fig. S7) showed spatially structured changes in the areas with higher reindeer activity on the erect shrub slope. These changes included larger height decreases where there were erect shrubs and increases between the shrubs. Even if these changes were robust, they do not necessarily imply that they would have consequences for future years, although they do provide evidence that they were not immediately

supplanted by vegetation growth during the peak growing season. In contrast, areas within the same habitat type but with lower reindeer activity had only low magnitude and less spatially structured changes. The lack of significance of the spatially structured changes suggests that the method for assigning significance we present here may be too conservative and that future work should consider adapting it to incorporate spatial awareness, rather than treating every pixel individually.

Our methodology can be developed further not only to quantify changes in canopy height, but also to derive measurements of biomass change, although it is important to consider uncertainty stemming from whether canopy height changes represent biomass removal or other physical impacts, as already mentioned. There is a strong, linear relationship between canopy height and aboveground biomass in non-forest ecosystems that is consistent within but different between plant functional types (Cunliffe et al., 2022). Thus, converting canopy height estimates into biomass would require additionally mapping plant functional types and ideally site-specific calibration of linear models using vegetation harvests and/or the point intercept method (Bråthen & Hagberg, 2004). This approach would also benefit from precise measurement of the terrain elevation using LiDAR to derive more reliable canopy height models (Alonzo et al., 2020). To quantify all biomass change, the LoD needs to be minimised across the study area to maximise the fine-scale changes that can be incorporated without capturing differences due to uncertainties stemming from the SfM processing. Although the changes we detected here were robust, they likely underestimate the total amount of change that occurred across the landscape, particularly in areas with a higher LoD such as tall vegetation patches as mentioned above. A larger quantity of precisely located ground control points or the use of drones with an onboard GNSS RTK receiver would better constrain the photogrammetric modelling, and higher-resolution drone

surveys capturing the vegetation from many angles in still conditions would enable rasterisation at finer resolution, reducing the DSM roughness (Graham et al., 2021; James et al., 2020). These improvements in survey quality would minimise the LoD, and the subsequent biomass calculations could then be used to determine, for example, the amount of biomass removed by grazing and browsing during an herbivory event.

Combining this measurement of animals' consumption with data on their movements opens the possibility for developing a more complete understanding of reindeer energetics (Trondrud et al., 2021). This would entail inferring a budget from simultaneous data on biomass consumed, derived from biomass removed from the site, and energy expenditure during movement, using some assumptions regarding metabolic rate. In this study, we used GPS collar data, which provide the opportunity to study animals' resource use, home range, and dispersal (Cagnacci et al., 2010) and has been employed to analyse, for example, reindeer summer habitat preferences and responses to built infrastructure (Skarin et al., 2008, 2018). However, the limited prior work using GPS collar data to quantify reindeer herbivory impacts over space utilised data with GPS location precision >100 m (Campeau et al., 2019; Rickbeil et al., 2015). Animal location data with metre-level precision, as we have used here, or at even finer spatio-temporal scales like those offered by emerging computer vision approaches (Koger et al., 2023), are necessary to assess vegetation responses to herbivory at the landscape scale and link reindeer consumption with energy expenditure.

Our findings are consistent with the widely observed ability of reindeer herbivory to limit deciduous shrub growth and maintain or enhance grasslands (Olofsson & Post, 2018). This effect was visible after a single herbivory pulse within a single growing season, but only where there was high reindeer activity and evidence of reindeer grazing, browsing, and trampling following

the herd's departure. By mapping vegetation responses continuously over space and analysing them within the context of the landscape, we were able to differentiate between the impacts of reindeer within different habitat and vegetation types, as well as identify where changes were likely unrelated to the herbivory event (Fig. 2,5). Whereas prior studies of top-down impacts on vegetation in the Arctic have employed remote sensing primarily to assess broader scale responses (Fauchald et al., 2017; Jefferies et al., 2006; Newton et al., 2014; Olofsson et al., 2012; Spiegel et al., 2023), our work demonstrates the value of very high-resolution, spatially continuous observations at the landscape scale for understanding the heterogeneity that is often present but difficult to characterise in traditional plot-based studies. Vegetation changes were heterogeneous in our study area, but our method facilitated explanation of that heterogeneity as linked to the interactions between reindeer herbivory pressure and habitat type, revealing how herbivory can shape the vegetation communities within a landscape. Our study design and processing workflows can be adapted to analyse vegetation change in a wide range of settings, including experiments such as those incorporating exclosures or fences, but also with other drivers, such as fires, if they can be mapped precisely over space. When combined with spatially explicit measurements, fine-scale remote sensing opens the opportunity to disentangle the interacting mechanisms controlling vegetation responses across different ecosystems at ecologically relevant scales.

Acknowledgements

We thank the Nenets family of Efim Serotetto for partnering with us and coordinating logistics to make this research possible. This study received funding and support from INTERACT III under the European Union H2020 Grant Agreement No. 871120 (to M.P.S); the EU-CHARTER project of the European Union's Horizon 2020 research and innovation programme under Grant

Agreement No. 869471 (to M.P.S., J.T.K., D.E., and M.M.-F.); the Russian Ministry of Science and Higher Education Program "Terrestrial ecosystems of northwestern Siberia: assessment of the modern transformation of the communities," No. 122021000089-9 (to A.V., A.T., V.F., K.S., N.S., and A.A.S.); and the Russian Science Foundation project No. 22–24-00642 (to A.T., V.F., and A.A.S.). M.P.S. was financially supported during the completion of this research by a Clarendon Scholarship from the University of Oxford. J.T.K acknowledges support from the European Union's Horizon research and innovation program under the Marie Sklodowska-Curie grant agreement No. 754513 and the Aarhus University Research Foundation.

Author Contributions

M.P.S., D.E., A.V., A.T., A.A.S., and M.M.-F. conceptualised the study and designed the methodology; D.E., A.V., A.T., N.S., and A.A.S. coordinated the logistics; M.P.S., D.E., and A.V. performed the data collection in the field; V.F. and K.S. contributed and analysed the GPS collar data; M.P.S. and J.T.K. processed and analysed the imagery; M.P.S., J.T.K., and M.M.-F. interpreted the results and created the figures; M.P.S. led the writing of the manuscript with significant contributions from all authors.

References

Alonzo, M., Dial, R. J., Schulz, B. K., Andersen, H.-E., Lewis-Clark, E., Cook, B. D., & Morton, D. C. (2020). Mapping tall shrub biomass in Alaska at landscape scale using structure-from-motion photogrammetry and lidar. *Remote Sensing of Environment*, *245*(May 2019), 111841. https://doi.org/10.1016/j.rse.2020.111841

Arnold, T. A., & Emerson, J. W. (2011). Nonparametric Goodness-of-Fit Tests for Discrete Null Distributions. *The R Journal*, *3*(2), 34–39. https://doi.org/10.32614/RJ-2011-016

Assmann, J. J., Myers-Smith, I. H., Kerby, J. T., Cunliffe, A. M., & Daskalova, G. N. (2020). Drone data reveal heterogeneity in tundra greenness and phenology not captured by

satellites. *Environmental Research Letters*, *15*(12), 125002. https://doi.org/10.1088/1748-9326/abbf7d

Bernes, C., Bråthen, K. A., Forbes, B. C., Speed, J. D. M., & Moen, J. (2015). What are the impacts of reindeer/caribou (Rangifer tarandus L.) on arctic and alpine vegetation? A systematic review. *Environmental Evidence*, *4*(4). https://doi.org/10.1186/s13750-014-0030-3

Bråthen, K. A., & Hagberg, O. (2004). More efficient estimation of plant biomass. *Journal of Vegetation Science*, *15*(5), 653–660. https://doi.org/10.1111/j.1654-1103.2004.tb02307.x

Bråthen, K. A., Ims, R. A., Yoccoz, N. G., Fauchald, P., Tveraa, T., & Hausner, V. H. (2007). Induced shift in ecosystem productivity? Extensive scale effects of abundant large herbivores. *Ecosystems*, *10*(5), 773–789. https://doi.org/10.1007/s10021-007-9058-3

Bråthen, K. A., Ravolainen, V. T., Stien, A., Tveraa, T., & Ims, R. A. (2017). Rangifer management controls a climate-sensitive tundra state transition. *Ecological Applications*, *27*(8), 2416–2427. https://doi.org/10.1002/eap.1618

Cagnacci, F., Boitani, L., Powell, R. A., & Boyce, M. S. (2010). Animal ecology meets GPS-based radiotelemetry: A perfect storm of opportunities and challenges. *Philosophical Transactions of the Royal Society B: Biological Sciences*, *365*(1550), 2157–2162. https://doi.org/10.1098/rstb.2010.0107

Campeau, A. B., Rickbeil, G. J. M., Coops, N. C., & Côté, S. D. (2019). Long-term changes in the primary productivity of migratory caribou (Rangifer tarandus) calving grounds and summer pasture on the Quebec-Labrador Peninsula (Northeastern Canada): the mixed influences of climate change and caribou herbivory. *Polar Biology*, *42*(5), 1005–1023. https://doi.org/10.1007/s00300-019-02492-6

Chapin III, F. S. (1980). Nutrient Allocation and Responses to Defoliation in Tundra Plants. *Arctic and Alpine Research*, *12*(4), 553. https://doi.org/10.2307/1550500

Chapin III, F. S., Johnson, D. A., & McKendrick, J. D. (1980). Seasonal Movement of Nutrients in Plants of Differing Growth Form in an Alaskan Tundra Ecosystem: Implications for Herbivory. *Journal of Ecology*, *68*(1), 189. https://doi.org/10.2307/2259251

Cohen, J., Pulliainen, J., Ménard, C. B., Johansen, B., Oksanen, L., Luojus, K., & Ikonen, J. (2013). Effect of reindeer grazing on snowmelt, albedo and energy balance based on satellite data analyses. *Remote Sensing of Environment*, *135*, 107–117. https://doi.org/10.1016/j.rse.2013.03.029

Colman, J. E., Eidesen, R., Hjermann, D., Gaup, M. A., Holand, Ø., Moe, S. R., & Reimers, E. (2004). Reindeer 24-hr within and between group synchronicity in summer versus environmental variables. *Rangifer*, *24*(1), 25–30. https://doi.org/10.7557/2.24.1.298

Cunliffe, A. M., Anderson, K., Boschetti, F., Brazier, R. E., Graham, H. A., Myers-Smith, I. H., Astor, T., Boer, M. M., Calvo, L. G., Clark, P. E., Cramer, M. D., Encinas-Lara, M. S.,

Escarzaga, S. M., Fernández-Guisuraga, J. M., Fisher, A. G., Gdulová, K., Gillespie, B. M., Griebel, A., Hanan, N. P., … Wojcikiewicz, R. (2022). Global application of an unoccupied aerial vehicle photogrammetry protocol for predicting aboveground biomass in non-forest ecosystems. *Remote Sensing in Ecology and Conservation*, *8*(1), 57–71. https://doi.org/10.1002/rse2.228

Cunliffe, A. M., Brazier, R. E., & Anderson, K. (2016). Ultra-fine grain landscape-scale quantification of dryland vegetation structure with drone-acquired structure-from-motion photogrammetry. *Remote Sensing of Environment*, *183*, 129–143. https://doi.org/10.1016/j.rse.2016.05.019

Cunliffe, A. M., J Assmann, J., N Daskalova, G., Kerby, J. T., & Myers-Smith, I. H. (2020). Aboveground biomass corresponds strongly with drone-derived canopy height but weakly with greenness (NDVI) in a shrub tundra landscape. *Environmental Research Letters*, *15*(12), 125004. https://doi.org/10.1088/1748-9326/aba470

Dandois, J. P., & Ellis, E. C. (2013). High spatial resolution three-dimensional mapping of vegetation spectral dynamics using computer vision. *Remote Sensing of Environment*, *136*, 259–276. https://doi.org/10.1016/j.rse.2013.04.005

Egelkraut, D., Aronsson, K.-Å., Allard, A., Åkerholm, M., Stark, S., & Olofsson, J. (2018). Multiple Feedbacks Contribute to a Centennial Legacy of Reindeer on Tundra Vegetation. *Ecosystems*, *21*(8), 1545–1563. https://doi.org/10.1007/s10021-018-0239-z

Egelkraut, D., Barthelemy, H., & Olofsson, J. (2020). Reindeer trampling promotes vegetation changes in tundra heathlands: Results from a simulation experiment. *Journal of Vegetation Science*, *31*(3), 476–486. https://doi.org/10.1111/jvs.12871

Ehrich, D., Henden, J.-A., Ims, R. A., Doronina, L. O., Killengren, S. T., Lecomte, N., Pokrovsky, I. G., Skogstad, G., Sokolov, A. A., Sokolov, V. A., & Yoccoz, N. G. (2012). The importance of willow thickets for ptarmigan and hares in shrub tundra: the more the better? *Oecologia*, *168*(1), 141–151. https://doi.org/10.1007/s00442-011-2059-0

Elmendorf, S. C., Henry, G. H. R., Hollister, R. D., Björk, R. G., Bjorkman, A. D., Callaghan, T. V., Collier, L. S., Cooper, E. J., Cornelissen, J. H. C., Day, T. A., Fosaa, A. M., Gould, W. A., Grétarsdóttir, J., Harte, J., Hermanutz, L., Hik, D. S., Hofgaard, A., Jarrad, F., Jónsdóttir, I. S., … Wookey, P. A. (2012). Global assessment of experimental climate warming on tundra vegetation: Heterogeneity over space and time. In *Ecology Letters* (Vol. 15, Issue 2, pp. 164–175). https://doi.org/10.1111/j.1461-0248.2011.01716.x

Epstein, H. E., Beringer, J., Gould, W. A., Lloyd, A. H., Thompson, C. D., Chapin, F. S., Michaelson, G. J., Ping, C. L., Rupp, T. S., & Walker, D. A. (2004). The nature of spatial transitions in the Arctic. *Journal of Biogeography*, *31*(12), 1917–1933. https://doi.org/10.1111/j.1365-2699.2004.01140.x

Fauchald, P., Park, T., Tømmervik, H., Myneni, R., & Hausner, V. H. (2017). Arctic greening from warming promotes declines in caribou populations. *Science Advances*, *3*(4). https://doi.org/10.1126/sciadv.1601365

Forbes, B. C., Stammler, F., Kumpula, T., Meschtyb, N., Pajunen, A., & Kaarlejärvi, E. (2009). High resilience in the Yamal-Nenets social-ecological system, West Siberian Arctic, Russia. *Proceedings of the National Academy of Sciences*, *106*(52), 22041–22048. https://doi.org/10.1073/pnas.0908286106

Fraser, R. H., Olthof, I., Lantz, T. C., & Schmitt, C. (2016). UAV photogrammetry for mapping vegetation in the low-Arctic. *Arctic Science*, *2*(3), 79–102. https://doi.org/10.1139/as-2016-0008

Goetz, S., & Dubayah, R. (2011). Advances in remote sensing technology and implications for measuring and monitoring forest carbon stocks and change. *Carbon Management*, *2*(3), 231–244. https://doi.org/10.4155/cmt.11.18

Graham, H., Benaud, P., Cunliffe, A., Puttock, A., Anderson, K., Chant, J., Elliott, M., & Brazier, R. (2021). *exeter-creww/SFM_Precision: SfM Precision and Workflow v0.2 (v0.2)*. Zenodo. https://doi.org/10.5281/zenodo.5760603

Greaves, H. E., Vierling, L. A., Eitel, J. U. H., Boelman, N. T., Magney, T. S., Prager, C. M., & Griffin, K. L. (2015). Estimating aboveground biomass and leaf area of low-stature Arctic shrubs with terrestrial LiDAR. *Remote Sensing of Environment*, *164*, 26–35. https://doi.org/10.1016/j.rse.2015.02.023

Habeck, J. O. (2007). *What it Means to be a Herdsman: The Practice and Image of Reindeer Husbandry*. Lit Verlag.

Hofhuis, S. P., Ehrich, D., Sokolova, N. A., van Hooft, P., & Sokolov, A. A. (2021). Breeding den selection by Arctic foxes (Vulpes lagopus) in southern Yamal Peninsula, Russia. *Polar Biology*, *44*(12), 2307–2319. https://doi.org/10.1007/s00300-021-02962-w

Istomin, K., & Dwyer, M. (2021). *Reindeer herder's thinking: A comparative research on relations between economy, cognition, and way of life*. Verlag der Kulturstiftung Sibirien.

James, M. R., Antoniazza, G., Robson, S., & Lane, S. N. (2020). Mitigating systematic error in topographic models for geomorphic change detection: accuracy, precision and considerations beyond off-nadir imagery. *Earth Surface Processes and Landforms*, *45*(10), 2251–2271. https://doi.org/10.1002/esp.4878

James, M. R., Robson, S., d'Oleire-Oltmanns, S., & Niethammer, U. (2017). Optimising UAV topographic surveys processed with structure-from-motion: Ground control quality, quantity and bundle adjustment. *Geomorphology*, *280*, 51–66. https://doi.org/10.1016/j.geomorph.2016.11.021

James, M. R., Robson, S., & Smith, M. W. (2017). 3-D uncertainty-based topographic change detection with structure-from-motion photogrammetry: precision maps for ground control

and directly georeferenced surveys. *Earth Surface Processes and Landforms*, *42*(12), 1769–1788. https://doi.org/10.1002/esp.4125

Jefferies, R. L., Jano, A. P., & Abraham, K. F. (2006). A biotic agent promotes large-scale catastrophic change in the coastal marshes of Hudson Bay. *Journal of Ecology*, *94*(1), 234–242. https://doi.org/10.1111/j.1365-2745.2005.01086.x

Jefferies, R. L., Klein, D. R., & Shaver, G. R. (1994). Vertebrate Herbivores and Northern Plant Communities: Reciprocal Influences and Responses. *Oikos*, *71*, 193–206. https://doi.org/10.2307/3546267

Jernsletten, J.-L. L., & Klokov, K. (2002). *Sustainable Reindeer Husbandry*.

Jung, T. S., Hegel, T. M., Bentzen, T. W., Egli, K., Jessup, L., Kienzler, M., Kuba, K., Kukka, P. M., Russell, K., Suitor, M. P., & Tatsumi, K. (2018). Accuracy and performance of low-feature GPS collars deployed on bison Bison bison and caribou Rangifer tarandus. *Wildlife Biology*, *2018*(1), 1–11. https://doi.org/10.2981/wlb.00404

Kaarlejärvi, E., Hoset, K. S., & Olofsson, J. (2015). Mammalian herbivores confer resilience of Arctic shrub-dominated ecosystems to changing climate. *Global Change Biology*, *21*(9), 3379–3388. https://doi.org/10.1111/gcb.12970

Karger, D. N., Conrad, O., Böhner, J., Kawohl, T., Kreft, H., Soria-Auza, R. W., Zimmermann, N. E., Linder, H. P., & Kessler, M. (2017). Climatologies at high resolution for the earth's land surface areas. *Scientific Data*, *4*, 1–20. https://doi.org/10.1038/sdata.2017.122

Karger, D. N., Conrad, O., Böhner, J., Kawohl, T., Kreft, H., Soria-Auza, R. W., Zimmermann, N. E., Linder, H. P., & Kessler, M. (2018). Climatologies at high resolution for the earth's land surface areas. *Dryad Digital Repository*. https://doi.org/10.5061/dryad.kd1d4

Koger, B., Deshpande, A., Kerby, J. T., Graving, J. M., Costelloe, B. R., & Couzin, I. D. (2023). Quantifying the movement, behaviour and environmental context of group-living animals using drones and computer vision. *Journal of Animal Ecology*, *92*(7), 1357–1371. https://doi.org/10.1111/1365-2656.13904

Macias-Fauria, M., Forbes, B. C., Zetterberg, P., & Kumpula, T. (2012). Eurasian Arctic greening reveals teleconnections and the potential for structurally novel ecosystems. *Nature Climate Change*, *2*, 613–618. https://doi.org/10.1038/nclimate1558

Myers-Smith, I. H., Elmendorf, S. C., Beck, P. S. A., Wilmking, M., Hallinger, M., Blok, D., Tape, K. D., Rayback, S. A., Macias-Fauria, M., Forbes, B. C., Speed, J. D. M., Boulanger-Lapointe, N., Rixen, C., Lévesque, E., Schmidt, N. M., Baittinger, C., Trant, A. J., Hermanutz, L., Collier, L. S., … Vellend, M. (2015). Climate sensitivity of shrub growth across the tundra biome. *Nature Climate Change*, *5*(9), 887–891. https://doi.org/10.1038/nclimate2697

Myers-Smith, I. H., Forbes, B. C., Wilmking, M., Hallinger, M., Lantz, T., Blok, D., Tape, K. D., MacIas-Fauria, M., Sass-Klaassen, U., Lévesque, E., Boudreau, S., Ropars, P., Hermanutz,

L., Trant, A., Collier, L. S., Weijers, S., Rozema, J., Rayback, S. A., Schmidt, N. M., … Hik, D. S. (2011). Shrub expansion in tundra ecosystems: Dynamics, impacts and research priorities. *Environmental Research Letters*, *6*(4). https://doi.org/10.1088/1748-9326/6/4/045509

Newton, E. J., Pond, B. A., Brown, G. S., Abraham, K. F., & Schaefer, J. A. (2014). Remote sensing reveals long-term effects of caribou on tundra vegetation. *Polar Biology*, *37*(5), 715–725. https://doi.org/10.1007/s00300-014-1472-3

Niittynen, P., Heikkinen, R. K., Aalto, J., Guisan, A., Kemppinen, J., & Luoto, M. (2020). Fine-scale tundra vegetation patterns are strongly related to winter thermal conditions. *Nature Climate Change*, *10*(12), 1143–1148. https://doi.org/10.1038/s41558-020-00916-4

Obu, J., Westermann, S., Bartsch, A., Berdnikov, N., Christiansen, H. H., Dashtseren, A., Delaloye, R., Elberling, B., Etzelmüller, B., Kholodov, A., Khomutov, A., Kääb, A., Leibman, M. O., Lewkowicz, A. G., Panda, S. K., Romanovsky, V., Way, R. G., Westergaard-Nielsen, A., Wu, T., … Zou, D. (2019). Northern Hemisphere permafrost map based on TTOP modelling for 2000–2016 at 1 km2 scale. *Earth-Science Reviews*, *193*, 299–316. https://doi.org/10.1016/j.earscirev.2019.04.023

Olofsson, J., Kitti, H., Rautiainen, P., Stark, S., & Oksanen, L. (2001). Effects of summer grazing by reindeer on composition of vegetation, productivity and nitrogen cycling. *Ecography*, *24*(1), 13–24. https://doi.org/10.1034/j.1600-0587.2001.240103.x

Olofsson, J., Oksanen, L., Callaghan, T., Hulme, P. E., Oksanen, T., & Suominen, O. (2009). Herbivores inhibit climate-driven shrub expansion on the tundra. *Global Change Biology*, *15*(11), 2681–2693. https://doi.org/10.1111/j.1365-2486.2009.01935.x

Olofsson, J., & Post, E. (2018). Effects of large herbivores on tundra vegetation in a changing climate, and implications for rewilding. *Philosophical Transactions of the Royal Society B: Biological Sciences*, *373*(1761). https://doi.org/10.1098/rstb.2017.0437

Olofsson, J., Stark, S., & Oksanen, L. (2004). Reindeer influence on ecosystem processes in the tundra. *Oikos*, *105*(2), 386–396. https://doi.org/10.1111/j.0030-1299.2004.13048.x

Olofsson, J., te Beest, M., & Ericson, L. (2013). Complex biotic interactions drive long-term vegetation dynamics in a subarctic ecosystem. *Philosophical Transactions of the Royal Society B: Biological Sciences*, *368*(1624), 20120486. https://doi.org/10.1098/rstb.2012.0486

Olofsson, J., Tommervik, H., & Callaghan, T. V. (2012). Vole and lemming activity observed from space. *Nature Climate Change*, *2*(12), 880–883. https://doi.org/10.1038/nclimate1537

Orndahl, K. M., Ehlers, L. P. W., Herriges, J. D., Pernick, R. E., Hebblewhite, M., & Goetz, S. J. (2022). Mapping tundra ecosystem plant functional type cover, height and aboveground biomass in Alaska and northwest Canada using unmanned aerial vehicles. *Arctic Science*, *1180*, 1165–1180. https://doi.org/10.1139/as-2021-0044

Over, J.-S. R., Ritchie, A. C., Kranenburg, C. J., Brown, J. A., Buscombe, D. D., Noble, T., Sherwood, C. R., Warrick, J. A., & Wernette, P. A. (2021). Processing coastal imagery with Agisoft Metashape Professional Edition, version 1.6—Structure from motion workflow documentation. In *U.S. Geological Survey Open-File Report*. https://doi.org/10.3133/ofr20211039

Petersen, T. K., Kolstad, A. L., Kouki, J., Leroux, S. J., Potvin, L. R., Tremblay, J. P., Wallgren, M., Widemo, F., Cromsigt, J. P. G. M., Courtois, C., Austrheim, G., Gosse, J., den Herder, M., Hermanutz, L., & Speed, J. D. M. (2023). Airborne laser scanning reveals uniform responses of forest structure to moose (Alces alces) across the boreal forest biome. *Journal of Ecology*, *111*(7), 1396–1410. https://doi.org/10.1111/1365-2745.14093

Post, E., Cahoon, S. M. P., Kerby, J. T., Pedersen, C., & Sullivan, P. F. (2021). Herbivory and warming interact in opposing patterns of covariation between arctic shrub species at large and local scales. *Proceedings of the National Academy of Sciences*, *118*(6), e2015158118. https://doi.org/10.1073/pnas.2015158118

Räsänen, A., & Virtanen, T. (2019). Data and resolution requirements in mapping vegetation in spatially heterogeneous landscapes. *Remote Sensing of Environment*, *230*(May), 111207. https://doi.org/10.1016/j.rse.2019.05.026

Raynolds, M. K., Walker, D. A., Epstein, H. E., Pinzon, J. E., & Tucker, C. J. (2012). A new estimate of tundra-biome phytomass from trans-Arctic field data and AVHRR NDVI. *Remote Sensing Letters*, *3*, 403–411. https://doi.org/10.1080/01431161.2011.609188

Rees, W. G., Williams, M., & Vitebsky, P. (2003). Mapping land cover change in a reindeer herding area of the Russian arctic using Landsat TM and ETM+ imagery and indigenous knowledge. *Remote Sensing of Environment*, *85*(4), 441–452. https://doi.org/10.1016/S0034-4257(03)00037-3

Rickbeil, G. J. M., Coops, N. C., & Adamczewski, J. (2015). The grazing impacts of four barren ground caribou herds (Rangifer tarandus groenlandicus) on their summer ranges: An application of archived remotely sensed vegetation productivity data. *Remote Sensing of Environment*, *164*, 314–323. https://doi.org/10.1016/j.rse.2015.04.006

Roussel, J.-R., & Auty, D. (2021). *Airborne LiDAR Data Manipulation and Visualization for Forestry Applications*.

Roussel, J.-R., Auty, D., Coops, N. C., Tompalski, P., Goodbody, T. R. H., Meador, A. S., Bourdon, J.-F., de Boissieu, F., & Achim, A. (2020). lidR: An R package for analysis of Airborne Laser Scanning (ALS) data. *Remote Sensing of Environment*, *251*, 112061. https://doi.org/10.1016/j.rse.2020.112061

Senft, R. L., Coughenour, M. B., Bailey, D. W., Rittenhouse, L. R., Sala, O. E., & Swift, D. M. (1987). Large Herbivore Foraging and Ecological Hierarchies. *BioScience*, *37*(11), 789–799. https://doi.org/10.2307/1310545

Siewert, M. B., & Olofsson, J. (2020). Scale-dependency of Arctic ecosystem properties revealed by UAV. *Environmental Research Letters*, *15*(9), 094030. https://doi.org/10.1088/1748-9326/aba20b

Siewert, M. B., & Olofsson, J. (2021). UAV reveals substantial but heterogeneous effects of herbivores on Arctic vegetation. *Scientific Reports*, *11*(1), 19468. https://doi.org/10.1038/s41598-021-98497-5

Skarin, A., Danell, Ö., Bergström, R., & Moen, J. (2008). Summer habitat preferences of GPS-collared reindeer Rangifer tarandus tarandus. *Wildlife Biology*, *14*(1), 1–15. https://doi.org/10.2981/0909-6396(2008)14[1:SHPOGR]2.0.CO;2

Skarin, A., Sandström, P., & Alam, M. (2018). Out of sight of wind turbines—Reindeer response to wind farms in operation. *Ecology and Evolution*, *8*(19), 9906–9919. https://doi.org/10.1002/ece3.4476

Skarin, A., Verdonen, M., Kumpula, T., Macias-Fauria, M., Alam, M., Kerby, J., & Forbes, B. C. (2020). Reindeer use of low Arctic tundra correlates with landscape structure. *Environmental Research Letters*, *15*(11), 115012. https://doi.org/10.1088/1748-9326/abbf15

Sokolov, A. A., Sokolova, N. A., Ims, R. A., Brucker, L., & Ehrich, D. (2016). Emergent Rainy Winter Warm Spells May Promote Boreal Predator Expansion into the Arctic. *ARCTIC*, *69*(2), 121–129. https://doi.org/10.14430/arctic4559

Sokolov, V., Ehrich, D., Yoccoz, N. G., Sokolov, A., & Lecomte, N. (2012). Bird Communities of the Arctic Shrub Tundra of Yamal: Habitat Specialists and Generalists. *PLoS ONE*, *7*(12), e50335. https://doi.org/10.1371/journal.pone.0050335

Sokolova, N. A., Sokolov, A. A., Ims, R. A., Skogstad, G., Lecomte, N., Sokolov, V. A., Yoccoz, N. G., & Ehrich, D. (2014). Small rodents in the shrub tundra of Yamal (Russia): Density dependence in habitat use? *Mammalian Biology*, *79*(5), 306–312. https://doi.org/10.1016/j.mambio.2014.04.004

Spiegel, M. P., Volkovitskiy, A., Terekhina, A., Forbes, B. C., Park, T., & Macias-Fauria, M. (2023). Top-Down Regulation by a Reindeer Herding System Limits Climate-Driven Arctic Vegetation Change at a Regional Scale. *Earth's Future*, *11*(7). https://doi.org/10.1029/2022EF003407

Stammler, F. (2005). *Reindeer Nomads Meet the Market: Culture, Property and Globalisation at the `End of the Land'*. Lit.

Stark, S., Horstkotte, T., Kumpula, J., Olofsson, J., Tømmervik, H., & Turunen, M. (2023). The ecosystem effects of reindeer (Rangifer tarandus) in northern Fennoscandia: Past, present and future. *Perspectives in Plant Ecology, Evolution and Systematics*, *58*, 125716. https://doi.org/10.1016/j.ppees.2022.125716

Sturm, M., Holmgren, J., McFadden, J. P., Liston, G. E., Chapin, F. S., & Racine, C. H. (2001). Snow-Shrub Interactions in Arctic Tundra: A Hypothesis with Climatic Implications.

Journal of Climate, *14*(3), 336–344. https://doi.org/10.1175/1520-0442(2001)014<0336:SSIIAT>2.0.CO;2

Sundqvist, M. K., Moen, J., Björk, R. G., Vowles, T., Kytöviita, M. M., Parsons, M. A., & Olofsson, J. (2019). Experimental evidence of the long-term effects of reindeer on Arctic vegetation greenness and species richness at a larger landscape scale. *Journal of Ecology*, *April*, 1–13. https://doi.org/10.1111/1365-2745.13201

Suvanto, S., Le Roux, P. C., & Luoto, M. (2014). Arctic-alpine vegetation biomass is driven by fine-scale abiotic heterogeneity. *Geografiska Annaler: Series A, Physical Geography*, *96*(4), n/a-n/a. https://doi.org/10.1111/geoa.12050

Te Beest, M., Sitters, J., Ménard, C. B., & Olofsson, J. (2016). Reindeer grazing increases summer albedo by reducing shrub abundance in Arctic tundra. *Environmental Research Letters*, *11*(12). https://doi.org/10.1088/1748-9326/aa5128

Terekhina, A., Filippova, V., Volkovitskiy, A., Shklyar, K., Orekhov, P., Sokolova, N., Abdulmanova, S., & Sokolov, A. (2022). Influence of Indigenous Herding Activities on the Spatio-temporal Distribution of Reindeer during the Summer-Autumn Period: Case from Yamal, Russia. *Human Ecology*. https://doi.org/10.1007/s10745-022-00384-8

Terekhina, A., & Volkovitskiy, A. (2020). Patterns of resource use by the Yamal nomads: The micro-regions ethnography. In V. N. Davydov (Ed.), *Energy of the Arctic and Siberia: The Use of Resources in the Context of Socio-Economic Changes* (pp. 87–113). Izdatel'stvo vostochnoi literatury.

Thomson, E. R., Spiegel, M. P., Althuizen, I. H. J., Bass, P., Chen, S., Chmurzynski, A., Halbritter, A. H., Henn, J. J., Jónsdóttir, I. S., Klanderud, K., Li, Y., Maitner, B. S., Michaletz, S. T., Niittynen, P., Roos, R. E., Telford, R. J., Enquist, B. J., Vandvik, V., Macias-Fauria, M., & Malhi, Y. (2021). Multiscale mapping of plant functional groups and plant traits in the High Arctic using field spectroscopy, UAV imagery and Sentinel-2A data. *Environmental Research Letters*, *16*(5). https://doi.org/10.1088/1748-9326/abf464

Trondrud, L. M., Pigeon, G., Albon, S., Arnold, W., Evans, A. L., Irvine, R. J., Król, E., Ropstad, E., Stien, A., Veiberg, V., Speakman, J. R., & Loe, L. E. (2021). Determinants of heart rate in Svalbard reindeer reveal mechanisms of seasonal energy management. *Philosophical Transactions of the Royal Society B: Biological Sciences*, *376*(1831), 20200215. https://doi.org/10.1098/rstb.2020.0215

Tuomi, M., Väisänen, M., Ylänne, H., Brearley, F. Q., Barrio, I. C., Anne Bråthen, K., Eischeid, I., Forbes, B. C., Jónsdóttir, I. S., Kolstad, A. L., Macek, P., Petit Bon, M., Speed, J. D. M., Stark, S., Svavarsdóttir, K., Thórsson, J., & Bueno, C. G. (2020). Stomping in silence: Conceptualizing trampling effects on soils in polar tundra. *Functional Ecology*, *February*, 1365-2435.13719. https://doi.org/10.1111/1365-2435.13719

Väisänen, M., Ylänne, H., Kaarlejärvi, E., Sjögersten, S., Olofsson, J., Crout, N., & Stark, S. (2014). Consequences of warming on tundra carbon balance determined by reindeer grazing history. *Nature Climate Change*, *4*(5), 384–388. https://doi.org/10.1038/nclimate2147

van der Wal, R. (2006). Do herbivores cause habitat degradation or vegetation state transition? Evidence from the tundra. *Oikos*, *114*(1), 177–186. https://doi.org/10.1111/j.2006.0030-1299.14264.x

Villoslada, M., Ylänne, H., Juutinen, S., Kolari, T. H. M., Korpelainen, P., Tahvanainen, T., Wolff, F., & Kumpula, T. (2023). Reindeer control over shrubification in subarctic wetlands: spatial analysis based on unoccupied aerial vehicle imagery. *Remote Sensing in Ecology and Conservation*, *9*(5), 687–706. https://doi.org/10.1002/rse2.337

Walker, D. A., Leibman, M. O., Epstein, H. E., Forbes, B. C., Bhatt, U. S., Raynolds, M. K., Comiso, J. C., Gubarkov, A. A., Khomutov, A. V., Jia, G. J., Kaarlejärvi, E., Kaplan, J. O., Kumpula, T., Kuss, P., Matyshak, G., Moskalenko, N. G., Orekhov, P., Romanovsky, V. E., Ukraientseva, N. G., & Yu, Q. (2009). Spatial and temporal patterns of greenness on the Yamal Peninsula, Russia: interactions of ecological and social factors affecting the Arctic normalized difference vegetation index. *Environmental Research Letters*, *4*(4), 045004. https://doi.org/10.1088/1748-9326/4/4/045004

Walker, D. A., Raynolds, M. K., Daniëls, F. J. A., Einarsson, E., Elvebakk, A., Gould, W. A., Katenin, A. E., Kholod, S. S., Markon, C. J., Melnikov, E. S., Moskalenko, N. G., Talbot, S. S., Yurtsev, B. A., & The other members of the CAVM Team. (2005). The Circumpolar Arctic vegetation map. *Journal of Vegetation Science*, *16*(3), 267–282. https://doi.org/10.1111/j.1654-1103.2005.tb02365.x

Wookey, P. A., Aerts, R., Bardgett, R. D., Baptist, F., Bråthen, K., Cornelissen, J. H. C., Gough, L., Hartley, I. P., Hopkins, D. W., Lavorel, S., & Shaver, G. R. (2009). Ecosystem feedbacks and cascade processes: Understanding their role in the responses of Arctic and alpine ecosystems to environmental change. *Global Change Biology*, *15*(5), 1153–1172. https://doi.org/10.1111/j.1365-2486.2008.01801.x

Yang, D., Morrison, B. D., Hantson, W., Breen, A. L., McMahon, A., Li, Q., Salmon, V. G., Hayes, D. J., & Serbin, S. P. (2021). Landscape-scale characterization of Arctic tundra vegetation composition, structure, and function with a multi-sensor unoccupied aerial system. *Environmental Research Letters*, *16*(8), 085005. https://doi.org/10.1088/1748-9326/ac1291

Zhang, W., Qi, J., Wan, P., Wang, H., Xie, D., Wang, X., & Yan, G. (2016). An Easy-to-Use Airborne LiDAR Data Filtering Method Based on Cloth Simulation. *Remote Sensing*, *8*(6), 501. https://doi.org/10.3390/rs8060501